

# Barrier-Certified Adaptive Reinforcement Learning with Applications to Brushbot Navigation

Motoya Ohnishi, *Student Member, IEEE*, Li Wang, *Member, IEEE*,  
Gennaro Notomista, *Student Member, IEEE*, and Magnus Egerstedt, *Fellow, IEEE*

**Abstract**— This paper presents a safe learning framework that employs an adaptive model learning method together with barrier certificates for systems with possibly nonstationary agent dynamics. To extract the dynamic structure of the model, we use a sparse optimization technique, and the resulting model will be used in combination with control barrier certificates which constrain policies (feedback controllers) in order to maintain safety, which refers to avoiding certain regions of the state space. Under certain conditions, recovery of safety in the sense of Lyapunov stability after violations of safety due to the nonstationarity is guaranteed. In addition, we reformulate action-value function approximation to make any kernel-based nonlinear function estimation method applicable to our adaptive learning framework. Lastly, solutions to the barrier-certified policy optimization are guaranteed to be globally optimal, ensuring greedy policy updates under mild conditions. The resulting framework is validated via simulations of a quadrotor, which has been used in the safe learnings literature under *stationarity* assumption, and then tested on a real robot called *brushbot*, whose dynamics is unknown, highly complex, and most probably nonstationary.

**Index Terms**— Safe learning, control barrier certificate, sparse optimization, kernel adaptive filter, brushbot

## I. INTRODUCTION

By exploring and interacting with an environment, reinforcement learning can successfully determine the optimal policy with respect to the long-term rewards given to an agent [1], [2]. Whereas the idea of determining the optimal policy in terms of a cost over some time horizon is standard in the controls literature [3], reinforcement learning is aimed at learning the long-term rewards by exploring the states and actions. As such, the agent dynamics is no longer explicitly taken into account, but rather is subsumed by the data. Moreover, even the rewards need not necessarily be known *a priori*, but can be obtained through exploration, as well.

If no information about the agent dynamics is available, however, an agent might end up in certain regions of the state space which must be avoided while exploring. Avoiding such regions of the state space is referred to as *safety*. Safety includes collision avoidance, boundary-transgression avoidance,

connectivity maintenance in teams of mobile robots, and other mandatory constraints, and this tension between exploration and safety becomes particularly pronounced in robotics, where safety is crucial.

In this paper, we address this safety issue, by employing model learning in combination with barrier certificates. In particular, we focus on learning for systems with discrete-time nonstationary agent dynamics. Nonstationarity comes, for example, from failures of actuators, battery degradations, or sudden environmental disturbances. The result is a method that adapts to a nonstationary agent dynamics and simultaneously extracts the dynamic structure without having to know how the agent dynamics changes over time. The resulting model will be used for barrier certificates. Under certain conditions, safety is recovered in the sense of Lyapunov stability even after violations of safety due to the nonstationarity occur. Moreover, we propose discrete-time barrier certificates with which a greedy policy update is ensured.

Over the last decade, the safety issue has been addressed under the name of safe learning, and plenty of solutions have been proposed [4]–[13]. To ensure safety while exploring, an initial knowledge of the agent dynamics, some safe maneuver or their long-term rewards, or a *teacher* advising the agent is necessary [4], [14]. To obtain a model of the agent dynamics, human operators may maneuver the agent and record its trajectories [12], [15], or, starting from an initial safe maneuver, the set of safe policies can be expanded by exploring the states [4], [5]. It is also possible that an agent continues exploring without entering the states with low long-term rewards associated with some safe maneuver (e.g., [16]). Due to the inherent uncertainty, the worst case scenario (e.g., possible lowest rewards) is typically taken into account when expanding the set of safe policies [13], [17]. To address the issue of this uncertainty for nonlinear-model estimation tasks, Gaussian process regression [18] is a strong tool, and many safe learning studies have taken advantage of its property (e.g., [4], [6], [7], [10], [13]).

Nevertheless, when the agent dynamics is nonstationary, the assumptions often made in the safe learning literature cannot hold any more. In such cases, strictly guaranteeing safety is unrealistic. For nonstationary agent dynamics, stable tracking of the agent dynamics for mitigating the negative effect of an unexpected violation of safety is desirable. Moreover, the long-term rewards must also be learned in an adaptive manner. These are the core motivations of this paper.

To constrain the states within a desired safe region, we employ control barrier functions (cf. [19]–[24]). When the

This work of M. Ohnishi was supported in part by the Scandinavia-Japan Sasakawa Foundation and the Travel Grant of the School of Electrical Engineering, KTH Royal Institute of Technology.

M. Ohnishi is with the School of Electrical Engineering, KTH Royal Institute of Technology, Stockholm, Sweden, the GRITS Lab, Georgia Institute of Technology, Atlanta, GA, USA, and also with the RIKEN Center for Advanced Intelligence Project, Tokyo, Japan (e-mail: motoya@kth.se).

L. Wang and M. Egerstedt are with the School of Electrical and Computer Engineering, Georgia Institute of Technology, Atlanta, GA, USA (e-mail: liwang@gatech.edu; magnus@gatech.edu).

G. Notomista is with the School of Mechanical Engineering, Georgia Institute of Technology, Atlanta, GA, USA (e-mail: g.notomista@gatech.edu).

exact model of the agent dynamics is available, control barrier certificates ensure that an agent remains in the set of safe states for all time by constraining the instantaneous control input at each time, and that an agent outside of the set of safe states is forced back to safety (Proposition III.1). A useful property of control barrier certificates is non-conservativeness, i.e., they modify policies when violations of safety are truly imminent. On the other hand, the global optimality of solutions to the constrained policy optimization is necessary to ensure the greedy improvement of a policy. Our first contribution of this paper is to propose a discrete-time control barrier certificate which ensures the global optimality under some mild conditions (see Section IV-C and Theorem IV.4 therein). This is an improvement of the previously proposed discrete-time control barrier certificate [24].

When the agent dynamics varies, the current estimate becomes no longer valid, possibly causing violations of safety. Therefore, we wish to adaptively learn the agent dynamics, and eventually bring the agent back to safety. To this end, we employ adaptive filtering techniques with stable tracking (or monotonic approximation) property: the current estimate is guaranteed to monotonically approach to the target system in the Hilbertian norm sense (see Section III-B). This guarantee is particularly important for safety-critical applications including robotics, and thus has high affinity to control theories. As the estimate becomes accurate, control barrier certificates will eventually force the agent back to the safe set hopefully before suffering from unrecoverable damages. In this paper, we employ a kernel adaptive filter [25] for *nonlinear* agent dynamics, which is an adaptive extension of the kernel ridge regression [26], [27] or Gaussian processes. Multikernel adaptive filter (cf. [28]–[32] and Appendix F) is a state-of-the-art kernel adaptive filter, which adaptively achieves a compact representation of a nonlinear function containing multi-component/partially-linear functions, and has a monotone approximation property for a possibly varying target function. Our second contribution of this paper is to guarantee Lyapunov stability of the safe set after the dynamics changes (Theorem IV.1), while adaptively learning the dynamic structure of the model by regarding a model of the agent dynamics as a combination of multiple structural components and employing a sparse optimization (see Section III-C and IV-B). The key idea is the use of an adaptive sparse optimization to extract truly *active* structural components.

Lastly, the action-value function, which approximates the long-term rewards, needs to be adaptively estimated under nonstationarity. Therefore, we wish to fully exploit the nonlinear adaptive filtering techniques. Actually, many attempts have been made to apply the online learning techniques to reinforcement learning (see [33]–[38]). As a result, so-called off-policy approaches, which are convergent even when samples are *not* generated by the target policy (see [34]), have been proposed. However, what differentiates action-value function approximation from an ordinary supervised learning, where input-output pairs are given, is that the output of the true action-value function is not explicitly observed. Our final contribution of this paper is, by assuming deterministic agent dynamics, to appropriately reformulate the action-value func-

tion approximation problem so that any kernel-based learning, which is widely-studied nonparametric technique, becomes straightforwardly applicable (Theorem IV.3).

To validate our learning framework and clarify each contribution, we first conduct simulations of a quadrotor. We then conduct real-robotics experiments on a *brushbot*, whose dynamics is unknown, highly complex, and most probably nonstationary, to test the efficacy of our framework (see Section V). This is challenging due to many uncertainties and lack of simulators often used in applications of reinforcement learning to robotics (see [39] for reinforcement learning in robotics).

## II. PRELIMINARIES

In this section, we present some of the related work and the system model considered in this paper. Throughout,  $\mathbb{R}$ ,  $\mathbb{Z}_{\geq 0}$ , and  $\mathbb{Z}_{>0}$  are the sets of real numbers, nonnegative integers, and positive integers, respectively. Let  $\|\cdot\|_{\mathcal{H}}$  be the norm induced by the inner product  $\langle \cdot, \cdot \rangle_{\mathcal{H}}$  in an inner-product space  $\mathcal{H}$ . In particular, define  $\langle \mathbf{x}, \mathbf{y} \rangle_{\mathbb{R}^L} := \mathbf{x}^T \mathbf{y}$  for  $L$ -dimensional real vectors  $\mathbf{x}, \mathbf{y} \in \mathbb{R}^L$ , and  $\|\mathbf{x}\|_{\mathbb{R}^L} := \sqrt{\langle \mathbf{x}, \mathbf{x} \rangle_{\mathbb{R}^L}}$ , where  $(\cdot)^T$  stands for transposition, and we let  $[\mathbf{x}; \mathbf{y}]$  denote  $[\mathbf{x}^T, \mathbf{y}^T]^T$ . Let  $\mathbf{x}_n \in \mathcal{X} \subset \mathbb{R}^{n_x}$  and  $\mathbf{u}_n \in \mathcal{U} \subset \mathbb{R}^{n_u}$  for  $n_x, n_u \in \mathbb{Z}_{>0}$  denote the state and the control input at time instant  $n \in \mathbb{R}_{\geq 0}$ , respectively.

### A. Related Work

The primary focus of this paper is the safety issue *while exploring*. Typically, some initial knowledges, such as an initial safe policy and a model of the agent dynamics, are required to address the safety issue while exploring, and model learning is often employed together. We introduce some related work on model learning and kernel-based action-value function approximation.

1) *Model Learning for Safe Maneuver*: The recent work in [13], [7], and [4] assumes an initial conservative set of safe policies, which is gradually expanded as more data become available. These approaches are designed for stationary agent dynamics, and Gaussian processes are employed to obtain the confidence interval of the model. To ensure safety, control barrier functions and control Lyapunov functions are employed in [13] and [4], respectively. On the other hand, the work in [10] uses a trajectory optimization based on the receding horizon control and model learning by Gaussian processes, which is computationally expensive when the model is highly nonlinear.

As analyzed in Section V-A later in this paper, Gaussian processes cannot adapt to the abrupt and unexpected change of the agent dynamics<sup>1</sup>. Hence, we employ an adaptive filter with monotone approximation property, which shares similar ideas with stable online learning for adaptive control based on Lyapunov stability (c.f. [40]–[43], for example).

<sup>1</sup>Although introducing forgetting factors will improve adaptivity, it is not straightforward to determine a suitable forgetting factor to guarantee any form of monotone approximation property under an *abrupt and unexpected change* of the agent dynamics.

2) *Learning Dynamic Structures in Reproducing Kernel Hilbert Spaces*: An approach that learns dynamics so as to the resulting model satisfies the Euler-Lagrange equation in reproducing kernel Hilbert spaces (RKHSs) was proposed in [44], while our paper proposes an adaptive learning of control-affine structure in RKHSs.

3) *Reinforcement Learning in Reproducing Kernel Hilbert Spaces*: We introduce, briefly, ideas of existing action-value function approximation techniques. Given a policy  $\phi : \mathcal{X} \rightarrow \mathcal{U}$ , the action-value function  $Q^\phi$  associated with the policy  $\phi$  is defined as

$$Q^\phi(\mathbf{x}, \phi(\mathbf{x})) = V^\phi(\mathbf{x}) := \sum_{n=0}^{\infty} \gamma^n R(\mathbf{x}_n, \phi(\mathbf{x}_n)), \quad (\text{II.1})$$

where  $\gamma \in (0, 1)$  is the discount factor,  $(\mathbf{x}_n)_{n \in \mathbb{Z}_{\geq 0}}$  is a trajectory of the agent starting from  $\mathbf{x}_0 = \mathbf{x}$ , and  $R(\mathbf{x}, \mathbf{u}) \in \mathbb{R}$  is the immediate reward. It is known that the action-value function follows the Bellman equation (c.f. [2, Equation (66)]):

$$Q^\phi(\mathbf{x}_n, \mathbf{u}_n) = \gamma Q^\phi(\mathbf{x}_{n+1}, \phi(\mathbf{x}_{n+1})) + R(\mathbf{x}_n, \mathbf{u}_n). \quad (\text{II.2})$$

If the state and control are in the grid world, an optimal policy can be obtained by a greedy search.

However, for robotics applications, where the states and controls are continuous, we need some form of function approximators to approximate the action-value function (and/or policies). Nonparametric learning such as a kernel method is often desirable when *a priori* knowledge about a suitable set of basis functions for learning is unavailable<sup>2</sup>. Kernel-based reinforcement learning has been studied in the literature, e.g., [35], [36], [36], [37], [46]–[56]. Although the outputs of the action-value function is unobserved, and supervised learning methods cannot be directly applied, so-called off-policy methods (e.g., the residual learning [33], the least squares temporal difference algorithm [57], and the gradient temporal difference learning [34], [58]) are proved to converge under certain conditions as most supervised learning methods even when samples are not generated by the policy  $\phi$ . The least squares temporal difference algorithm has been extended to kernel-based methods [37], including Gaussian processes (e.g., the Gaussian process temporal difference and the Gaussian process SARSA [35]).

In contrast to the aforementioned approaches, we explicitly define a so-called reproducing kernel Hilbert space so that action-value function approximation can be conducted as supervised learning in that space, rather than presenting an ad-hoc kernel-based algorithm for action-value function approximation. Consequently, any kernel-based method can be straightforwardly applied. The Gaussian process SARSA can also be reproduced by employing a Gaussian process in the explicitly defined RKHS as will be discussed in Appendix G. We can also conduct action-value function approximation in the same RKHS even after the agent dynamics changes or the policy is updated if an adaptive filter is employed in the RKHS (See the remark below Theorem IV.3) and Section V-A.2.

Specifically, in this paper, a possibly nonstationary agent dynamics is considered as described below.

<sup>2</sup>We refer the readers to [45] for a summary of *parametric* value function approximation techniques.

## B. System Model

In this paper, we consider the following discrete-time deterministic nonlinear model of the nonstationary agent dynamics,

$$\mathbf{x}_{n+1} - \mathbf{x}_n = p(\mathbf{x}_n, \mathbf{u}_n) + f(\mathbf{x}_n) + g(\mathbf{x}_n)\mathbf{u}_n, \quad (\text{II.3})$$

where  $p : \mathcal{X} \times \mathcal{U} \rightarrow \mathbb{R}^{n_x}$ ,  $f : \mathcal{X} \rightarrow \mathbb{R}^{n_x}$ ,  $g : \mathcal{X} \rightarrow \mathbb{R}^{n_x \times n_u}$  are continuous. Hereafter, we regard  $\mathcal{X} \times \mathcal{U}$  as the same as  $\mathcal{Z} \subset \mathbb{R}^{n_x+n_u}$  under the one-to-one correspondence between  $\mathbf{z} := [\mathbf{x}; \mathbf{u}] \in \mathcal{Z}$  and  $(\mathbf{x}, \mathbf{u}) \in \mathcal{X} \times \mathcal{U}$ , if there is no confusion.

We consider an agent with dynamics given in (II.3), and the goal is to find an optimal policy which drives the agent to a desirable state *while remaining in the set of safe states*  $\mathcal{C} \subset \mathcal{X}$  defined as

$$\mathcal{C} := \{\mathbf{x} \in \mathcal{X} \mid B(\mathbf{x}) \geq 0\}, \quad (\text{II.4})$$

where  $B : \mathcal{X} \rightarrow \mathbb{R}$ . An optimal policy is a policy  $\phi$  that attains an optimal value  $Q^\phi(\mathbf{x}, \phi(\mathbf{x}))$  for every state  $\mathbf{x} \in \mathcal{X}$ . Note that the value associated with a policy varies when the dynamics varies, and that a quadruple  $(\mathbf{x}_n, \mathbf{u}_n, \mathbf{x}_{n+1}, R(\mathbf{x}_n, \mathbf{u}_n))$  is available at each time instant  $n$ .

With these preliminaries in place, we can present the overview of our safe learning framework under possibly nonstationary dynamics.

## III. OVERVIEW OF THE SAFE LEARNING FRAMEWORK

When the agent dynamics varies abruptly and unexpectedly, safety cannot be no longer guaranteed. In this case, we at least wish to bring the agent back to safety. We introduce methods employed and extended in this paper, and present the motivations of using them here.

### A. Discrete-time Control Barrier Functions

In this paper, we employ control barrier functions to deal with safety issues. The idea of control barrier functions is similar to Lyapunov functions; they require no explicit computations of the forward reachable set while ensuring certain properties by constraining the instantaneous control input. Particularly, control barrier functions guarantee that an agent starting from the safe set remains safe (i.e., forward invariance), and that an agent outside of the safe set is forced back to safety (i.e., Lyapunov stability of the safe set) if the agent dynamics is available. To make the use of barrier certificate compatible with the model learning and reinforcement learning, we employ the discrete-time version of control barrier certificates.

**Definition III.1** ([24, Definition 4]). A map  $B : \mathcal{X} \rightarrow \mathbb{R}$  is a discrete-time exponential control barrier function if there exists a control input  $\mathbf{u}_n \in \mathcal{U}$  such that

$$B(\mathbf{x}_{n+1}) - B(\mathbf{x}_n) \geq -\eta B(\mathbf{x}_n), \quad \forall n \in \mathbb{Z}_{\geq 0}, \quad 0 < \eta \leq 1. \quad (\text{III.1})$$

Note that we intentionally removed the condition  $B(\mathbf{x}_0) \geq 0$  originally presented in [24, Definition 4]. Then, the forward invariance and asymptotic stability of the set of safe states are ensured by the following proposition.

**Proposition III.1.** The set  $\mathcal{C}$  defined in (II.4) for some discrete-time exponential control barrier function  $B: \mathcal{X} \rightarrow \mathbb{R}$  is forward invariant when  $B(\mathbf{x}_0) \geq 0$ , and is asymptotically stable when  $B(\mathbf{x}_0) < 0$ .

*Proof.* See [24, Proposition 4] for the proof of forward invariance. The set  $\mathcal{C} \subset \mathcal{X}$  is asymptotically stable as

$$\lim_{n \rightarrow \infty} B(\mathbf{x}_n) \geq \lim_{n \rightarrow \infty} (1 - \eta)^n B(\mathbf{x}_0) = 0,$$

where the inequality holds from [24, Proposition 1].  $\square$

Proposition III.1 implies that an agent remains in the set of safe states defined in (II.4) for all time if  $B(\mathbf{x}_0) \geq 0$  and (III.1) are satisfied, and the agent outside of the set of safe states is brought back to safety.

The main motivations of using control barrier functions are given below:

- a). Non-conservativeness, i.e., control barrier functions modify policies only when violations of safety are imminent. Consequently, an inaccurate or rough estimation of the model causes less negative effect on (model-free) reinforcement learning. This is not true for control Lyapunov functions, which enforce the decrease condition even inside the safe set. The differences between control barrier functions and control Lyapunov functions are well-analyzed in [59], for example.
- b). Asymptotic stability of the safe set, i.e., if the agent is outside of the safe set, it is brought back to the safe set. In addition to Proposition III.1, this robustness property is analyzed in [19]. This property together with adaptive model learning presented in the next subsection is particularly important when the nonstationarity of the dynamics pushes out the agent from the safe sets.

To enforce barrier certificates, we need a model of the agent dynamics, and for a possibly nonstationary agent dynamics, we need to *adaptively* learn the model.

### B. Adaptive Model Learning with Stable Tracking Property

At each time instant, an input-output pair  $(\mathbf{z}_n, \delta_n)$ , where  $\mathbf{z}_n := [\mathbf{x}_n; \mathbf{u}_n]$  and  $\delta_n := \mathbf{x}_{n+1} - \mathbf{x}_n$  for model learning is available. Under possibly nonstationary agent dynamics, it is vital for the model parameter estimation to be stable even after the agent dynamics changes. In this paper, we employ an adaptive learning with monotone approximation property. Note this approach shares the motivations of stable online learning with Lyapunov-like conditions.

Suppose that the estimate of model parameter at time instant  $n$  is given by  $\mathbf{h}_n \in \mathbb{R}^r$ ,  $r \in \mathbb{Z}_{>0}$ . Given a cost function  $\Theta_n(\mathbf{h})$  at time instant  $n$ , we update the parameter  $\mathbf{h}_n$  so as to satisfy the strictly monotone approximation property  $\|\mathbf{h}_{n+1} - \mathbf{h}_n^*\|_{\mathbb{R}^r} < \|\mathbf{h}_n - \mathbf{h}_n^*\|_{\mathbb{R}^r}$ ,  $\forall \mathbf{h}_n^* \in \Omega_n := \operatorname{argmin}_{\mathbf{h} \in \mathbb{R}^r} \Theta_n(\mathbf{h})$  if  $\mathbf{h}_n \notin \Omega_n \neq \emptyset$ , where  $\emptyset$  is the empty set. Under nonstationarity, this monotone approximation property tells that, no matter how the target vector(function) changes, we can at least guarantee that the current estimator  $\mathbf{h}_n$  gets closer to the current target vector.

Assume that  $\Omega := \bigcap_{n \in \mathbb{Z}_{\geq 0}} \Omega_n$  is nonempty. Then,  $\|\mathbf{h}_{n+1} - \mathbf{h}^*\|_{\mathbb{R}^r} < \|\mathbf{h}_n - \mathbf{h}^*\|_{\mathbb{R}^r}$ ,  $\forall \mathbf{h}^* \in \Omega$ ,  $n \in \mathbb{Z}_{\geq 0}$ , holds if  $\mathbf{h}_n \notin \Omega_n$ . This is illustrated in Figure III.1. This property

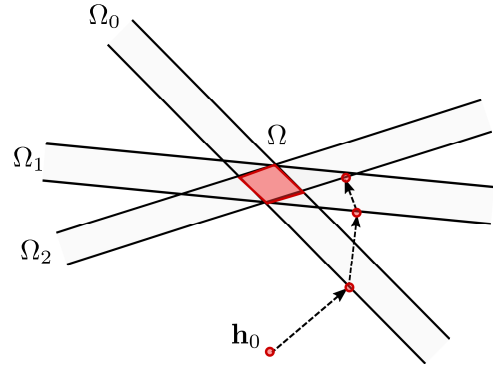


Fig. III.1. An illustration of monotone approximation property. The estimate  $\mathbf{h}_n$  monotonically approaches to the set  $\Omega$  of optimal vectors  $\mathbf{h}^*$  by sequentially minimizing the distance between  $\mathbf{h}_n$  and  $\Omega_n$ . Here,  $\Omega_n := \operatorname{argmin}_{\mathbf{h} \in \mathbb{R}^r} \Theta_n(\mathbf{h})$ , where  $\Theta_n(\mathbf{h})$  is the cost function at time instant  $n$ .

can also be viewed as Lyapunov stability of the model parameter. By augmenting the state vector with the model parameter, and by employing a suitable candidate of Lyapunov functions, we can thus guarantee that the agent is brought back to safety even after abrupt and unexpected changes of the agent dynamics (see Section IV-A).

For general nonlinear dynamics, we use a kernel adaptive filter with monotone approximation property. Due to its celebrated property of reproducing kernels, the framework of linear adaptive filter is directly applied to nonlinear function estimation tasks in a possibly infinite-dimensional functional space, namely a reproducing kernel Hilbert space.

**Definition III.2** ([60, page 343]). Given a nonempty set  $\mathcal{Z}$  and  $\mathcal{H}$  which is a Hilbert space defined in  $\mathcal{Z}$ , the function  $\kappa(\mathbf{z}, \mathbf{w})$  of  $\mathbf{z}, \mathbf{w} \in \mathcal{Z}$  is called a reproducing kernel of  $\mathcal{H}$  if

- 1) for every  $\mathbf{w} \in \mathcal{Z}$ ,  $\kappa(\mathbf{z}, \mathbf{w})$  as a function of  $\mathbf{z} \in \mathcal{Z}$  belongs to  $\mathcal{H}$ , and
- 2) it has the reproducing property, i.e., the following holds for every  $\mathbf{w} \in \mathcal{Z}$  and every  $\varphi \in \mathcal{H}$  that

$$\varphi(\mathbf{w}) = \langle \varphi, \kappa(\cdot, \mathbf{w}) \rangle_{\mathcal{H}}.$$

If  $\mathcal{H}$  has a reproducing kernel,  $\mathcal{H}$  is called a Reproducing Kernel Hilbert Space (RKHS).

One of the celebrated examples of kernels is the Gaussian kernel  $\kappa(\mathbf{x}, \mathbf{y}) := \frac{1}{(2\pi\sigma^2)^{L/2}} \exp\left(-\frac{\|\mathbf{x} - \mathbf{y}\|_{\mathbb{R}^L}^2}{2\sigma^2}\right)$ ,  $\mathbf{x}, \mathbf{y} \in \mathbb{R}^L$ ,  $\sigma > 0$ . It is well-known that the Gaussian reproducing kernel Hilbert space has universality [61], i.e., any continuous function on every compact subset of  $\mathbb{R}^L$  can be approximated with an arbitrary accuracy. Another widely used kernel is the polynomial kernel  $\kappa(\mathbf{x}, \mathbf{y}) := (\mathbf{x}^\top \mathbf{y} + c)^d$ ,  $c \geq 0, d \in \mathbb{Z}_{>0}$ .

We emphasize that monotone approximation property due to convexity of the formulations is the main motivation of using a kernel adaptive filter for adaptive model learning.

### C. Learning Dynamic Structure via Sparse Optimizations

To efficiently constrain policies by using control barrier functions, a dynamic structure called *control-affine* structure

is preferable (see Section IV-C and Theorem IV.4 therein). Control-affine dynamics is given by (II.3) when  $p = 0$ , where 0 denotes the null function. In practice, it is unrealistic to have completely control-affine model (i.e.,  $p = 0$ ) due to the effects of frictions and other disturbances. However, as long as the term  $p$  is negligibly small, we can consider the term  $p$  to be a *system noise* added to a control-affine system as discussed in Section IV-C and Theorem IV.4 therein, and we take the following steps to extract the control-affine structure:

- 1) Define  $\psi(\mathbf{x}, \mathbf{u}) := p(\mathbf{x}, \mathbf{u}) + f(\mathbf{x}) + g(\mathbf{x})\mathbf{u}$ , where  $\psi : \mathcal{X} \rightarrow \mathbb{R}$ .
- 2) Assume for simplicity that  $n_x = 1$ . We suppose that  $p \in \mathcal{H}_p$ ,  $f \in \mathcal{H}_f$ , and  $g^{(1)}, g^{(2)}, \dots, g^{(n_u)} \in \mathcal{H}_g$ , where  $\mathcal{H}_p$ ,  $\mathcal{H}_f$ , and  $\mathcal{H}_g$  are RKHSs, and  $g(\mathbf{x}) = [g^{(1)}(\mathbf{x}), g^{(2)}(\mathbf{x}), \dots, g^{(n_u)}(\mathbf{x})]$ .
- 3) Let  $\mathcal{H}_u$  be the RKHS associated with the reproducing kernel  $\kappa(\mathbf{u}, \mathbf{v}) := \mathbf{u}^T \mathbf{v}$ ,  $\mathbf{u}, \mathbf{v} \in \mathcal{U}$ , i.e., a polynomial kernel with  $c = 0$  and  $d = 1$ , and  $\mathcal{H}_c$  be the set of constant functions. Then, the function  $\psi$  can be estimated in the Hilbert space  $\mathcal{H}_\psi := \mathcal{H}_p + \mathcal{H}_f \otimes \mathcal{H}_c + \mathcal{H}_g \otimes \mathcal{H}_u$ . The Hilbert space  $\mathcal{H}_\psi$  is an RKHS (see Section IV-B and Theorem IV.2 therein), and hence we can employ a kernel adaptive filter.
- 4) Define the cost  $\Theta_n$  so as to promote sparsity of the model parameter. Consequently, we wish to obtain a control-affine model (i.e., the estimate of  $p$  denoted by  $\hat{p}$  becomes null) if the underlying true dynamics is control affine.

The resulting control-affine part of the estimated dynamics will be used in combination with the control barrier certificates in order to efficiently constrain policies so that the agent remains in the set of safe states and is stabilized on the set even after an abrupt and unexpected change of the agent dynamics while and after learning an optimal policy (see Theorem IV.1 and Theorem IV.4 for more details).

#### D. Adaptive Action-value Function Approximation in RKHSs

Lastly, we present barrier-certified action-value function approximation in RKHSs. One of the issues arising when applying a kernel method to action-value function approximation is that the output of the action-value function  $Q^\phi(\mathbf{x}_n, \mathbf{u}_n) \in \mathcal{H}_Q$  associated with a policy  $\phi$ , where  $\mathcal{H}_Q$  is assumed to be an RKHS, is unobservable. Nevertheless, we know that the action-value function follows the Bellman equation (II.2). Hence, by defining a function  $\psi^Q : \mathcal{X}^2 \rightarrow \mathbb{R}$ , where  $\mathbb{R}^{2(n_x+n_u)} \supset \mathcal{X}^2 = \mathcal{X} \times \mathcal{X}$ , as

$$\begin{aligned} \psi^Q([\mathbf{z}; \mathbf{w}]) &:= Q^\phi(\mathbf{x}, \mathbf{u}) - \gamma Q^\phi(\mathbf{y}, \mathbf{v}), \\ \mathbf{x}, \mathbf{y} \in \mathcal{X}, \mathbf{u}, \mathbf{v} \in \mathcal{U}, \mathbf{z} &= [\mathbf{x}; \mathbf{u}], \mathbf{w} = [\mathbf{y}; \mathbf{v}], \end{aligned}$$

the Bellman equation in (II.2) is solved via iterative nonlinear function estimation with the input-output pairs  $\{([\mathbf{x}_n; \mathbf{u}_n; \mathbf{x}_{n+1}; \phi(\mathbf{x}_{n+1})], R(\mathbf{x}_n, \mathbf{u}_n))\}_{n \in \mathbb{Z}_{\geq 0}}$ .

To theoretically guarantee the greedy improvement of policies, globally optimal control input within control constraints has to be taken at each state. Nevertheless, it is known that discrete-time barrier certificates become non-convex in general. Therefore, we will present certain conditions under which

the control constraint becomes convex in control (Section IV-C and Theorem IV.4 therein).

## IV. ANALYSIS OF BARRIER-CERTIFIED ADAPTIVE REINFORCEMENT LEARNING

In the previous section, we presented our barrier-certified adaptive reinforcement learning framework and the motivations of employing each method. In this section, we present theoretical analysis of our framework to further strengthen the arguments.

### A. Safety Recovery: Adaptive Learning and Control Barrier Certificates

Monotone approximation property of the model parameter is closely related to Lyapunov stability. In fact, by augmenting the state vector with the model parameter, we can construct a Lyapunov function which guarantees stability of the safe set under certain conditions.

We first make following assumptions.

- Assumption IV.1.**
- 1) The dimension of model parameter  $\mathbf{h}$  remains finite, and is  $r \in \mathbb{Z}_{>0}$ .
  - 2) The input space  $\mathcal{X}$  is invariant.
  - 3) All of the basis functions (or kernel functions) are bounded over  $\mathcal{X}$ .
  - 4) The control barrier function  $B$  is Lipschitz continuous over  $\mathcal{X}$  with Lipschitz constant  $v_B$ .
  - 5) There exist a control input  $\mathbf{u}_n \in \mathcal{U}$  satisfying for a sufficiently small  $\rho_1 > 0$  that

$$\begin{aligned} B(\hat{\mathbf{x}}_{n+1}) - B(\mathbf{x}_n) &\geq -\eta B(\mathbf{x}_n) + \rho_1, \\ \forall n \in \mathbb{Z}_{\geq 0}, 0 < \eta &\leq 1, \end{aligned} \quad (\text{IV.1})$$

where  $\hat{\mathbf{x}}_{n+1}$  is the predicted output of the current estimate  $\mathbf{h}_n$  at  $\mathbf{x}_n$  and  $\mathbf{u}_n$ .

- 6) If  $\mathbf{h}_n \in \Omega_n := \text{argmin}_{\mathbf{h} \in \mathbb{R}^r} \Theta_n(\mathbf{h})$ , where  $\Theta_n(\mathbf{h})$  is the cost function at time instant  $n$ , then  $\|\mathbf{x}_{n+1} - \hat{\mathbf{x}}_{n+1}\|_{\mathbb{R}^{n_x}} \leq \frac{\rho_1}{v_B}$ .

*Remark IV.1* (On Assumption IV.1.1). Assumption IV.1.1 is reasonable if polynomial kernels are employed for learning or if the input space  $\mathcal{X} := \mathcal{X} \times \mathcal{U}$  is compact.

*Remark IV.2* (On Assumption IV.1.5). Assumption IV.1.5 implies that we can enforce barrier certificates for the current estimate of the dynamics with a sufficiently small margin  $\rho_1$ . Although this assumption is somewhat restrictive, it is still reasonable if the initial estimate does not largely deviate from the true dynamics.

*Remark IV.3* (On Assumption IV.1.6). Assumption IV.1.6 implies that the set  $\Omega_n$  or equivalently the cost  $\Theta_n$  is designed so that the predicted output  $\hat{\mathbf{x}}_{n+1}$  for  $\mathbf{h}_n \in \Omega_n$  is sufficiently close to the true output  $\mathbf{x}_{n+1}$ , and this assumption is thus reasonable.

Let the augmented state be  $[\mathbf{x}; \mathbf{h}] \in \mathbb{R}^{n_x+r}$ . Then, the following theorem states that the safe set  $\mathcal{C}$  is (asymptotically) stable even after a violation of safety due to the abrupt and unexpected change of the agent dynamics.

**Theorem IV.1.** Suppose that a triple  $(\mathbf{x}_n, \mathbf{u}_n, \mathbf{x}_{n+1})$  is available at time instant  $n + 1$ , and the model parameter is updated as  $\mathbf{h}_{n+1} = T_n(\mathbf{h}_n)$ , where  $T_n : \mathbb{R}^r \rightarrow \mathbb{R}^r$  is continuous and has monotone approximation property: if  $\mathbf{h}_n \notin \Omega_n \neq \emptyset$ , then,  $\|\mathbf{h}_{n+1} - \mathbf{h}_n^*\|_{\mathbb{R}^r} \leq \rho_2 \|\mathbf{h}_n - \mathbf{h}_n^*\|_{\mathbb{R}^r}$ , for all  $\mathbf{h}_n^* \in \Omega_n := \operatorname{argmin}_{\mathbf{h} \in \mathbb{R}^r} \Theta_n(\mathbf{h})$ , and for some  $\rho_2 \in [0, 1)$ . Suppose also that the agent dynamics changes unexpectedly at time instant  $N_1 \in \mathbb{Z}_{>0}$ , and the set  $\Omega := \bigcap_{n \in \mathbb{Z}_{\geq N_1}} \Omega_n$  is nonempty. Then, under Assumption IV.1, the augmented safe set  $\mathcal{C} \times \Omega \subset \mathbb{R}^{n_x+r}$  is asymptotically stable if a control input  $\mathbf{u}_n$  satisfying (IV.1) is employed for all  $n \geq N_1$ , and if  $\mathbf{h}_n \notin \Omega_n$  for all  $n \geq N_1$  such that  $[\mathbf{x}_n; \mathbf{h}_n] \notin \mathcal{C} \times \Omega$ .

*Proof.* From Assumptions IV.1.3, IV.1.6, and the fact that the estimated output is linear to the model parameter for a fixed input, we obtain that

$$\|\mathbf{x}_{n+1} - \hat{\mathbf{x}}_{n+1}\|_{\mathbb{R}^{n_x}} - \frac{\rho_1}{v_B} \leq \rho_3 \operatorname{dist}(\mathbf{h}_n, \Omega_n),$$

for some bounded  $\rho_3 > 0$ . Therefore, from Assumption IV.1.4, we obtain

$$\begin{aligned} |B(\mathbf{x}_{n+1}) - B(\hat{\mathbf{x}}_{n+1})| - \rho_1 &\leq v_B \|\mathbf{x}_{n+1} - \hat{\mathbf{x}}_{n+1}\|_{\mathbb{R}^{n_x}} - \rho_1 \\ &\leq v_B \rho_3 \operatorname{dist}(\mathbf{h}_n, \Omega_n) \\ &\leq \frac{v_B \rho_3}{1 - \rho_2} [\operatorname{dist}(\mathbf{h}_n, \Omega) - \operatorname{dist}(\mathbf{h}_{n+1}, \Omega)], \end{aligned}$$

if  $\mathbf{h}_n \notin \Omega_n$ . If  $B(\mathbf{x}_{n+1}) < B(\hat{\mathbf{x}}_{n+1})$ , then we obtain

$$\begin{aligned} B(\mathbf{x}_{n+1}) - B(\hat{\mathbf{x}}_{n+1}) &\geq -\rho_1 - \frac{v_B \rho_3}{1 - \rho_2} [\operatorname{dist}(\mathbf{h}_n, \Omega) - \operatorname{dist}(\mathbf{h}_{n+1}, \Omega)]. \end{aligned} \quad (\text{IV.2})$$

This inequality also holds for the case that  $B(\mathbf{x}_{n+1}) \geq B(\hat{\mathbf{x}}_{n+1})$  and/or  $\mathbf{h}_n \in \Omega_n$ . We show that there exists a Lyapunov function  $V_{\mathcal{C} \times \Omega}$  for the augmented state  $[\mathbf{x}; \mathbf{h}]$ . A candidate function is given by

$$V_{\mathcal{C} \times \Omega}([\mathbf{x}; \mathbf{h}]) = \begin{cases} 0 & \text{if } [\mathbf{x}; \mathbf{h}] \in \mathcal{C} \times \Omega \\ -\min(B(\mathbf{x}), 0) + \frac{2v_B \rho_3}{1 - \rho_2} \operatorname{dist}(\mathbf{h}, \Omega) & \text{if } [\mathbf{x}; \mathbf{h}] \notin \mathcal{C} \times \Omega \end{cases}$$

Since  $-\min(B(\mathbf{x}), 0) + \frac{2v_B \rho_3}{1 - \rho_2} \operatorname{dist}(\mathbf{h}, \Omega) = 0$ ,  $\forall [\mathbf{x}; \mathbf{h}] \in \partial(\mathcal{C} \times \Omega)$ , where  $\partial(\mathcal{C} \times \Omega)$  is the boundary of the set  $\mathcal{C} \times \Omega$ , from Assumption IV.1.4, it follows that  $V_{\mathcal{C} \times \Omega}([\mathbf{x}; \mathbf{h}])$  is continuous. It also holds that  $V_{\mathcal{C} \times \Omega}([\mathbf{x}; \mathbf{h}]) > 0$  when  $[\mathbf{x}; \mathbf{h}] \notin \mathcal{C} \times \Omega$ , and that

$$\begin{aligned} &V_{\mathcal{C} \times \Omega}([\mathbf{x}_{n+1}; \mathbf{h}_{n+1}]) - V_{\mathcal{C} \times \Omega}([\mathbf{x}_n; \mathbf{h}_n]) \\ &= -\min(B(\mathbf{x}_{n+1}), 0) + \frac{2v_B \rho_3}{1 - \rho_2} \operatorname{dist}(\mathbf{h}_{n+1}, \Omega) \\ &+ \min(B(\mathbf{x}_n), 0) - \frac{2v_B \rho_3}{1 - \rho_2} \operatorname{dist}(\mathbf{h}_n, \Omega) \\ &\leq -\frac{v_B \rho_3}{1 - \rho_2} [\operatorname{dist}(\mathbf{h}_n, \Omega) - \operatorname{dist}(\mathbf{h}_{n+1}, \Omega)] \leq 0, \end{aligned} \quad (\text{IV.3})$$

for all  $n \geq N_1$ , where the first inequality follows because (IV.1) and (IV.2) yield

$$-\min(B(\mathbf{x}_{n+1}), 0) \leq \frac{v_B \rho_3}{1 - \rho_2} [\operatorname{dist}(\mathbf{h}_n, \Omega) - \operatorname{dist}(\mathbf{h}_{n+1}, \Omega)],$$

for  $B(\mathbf{x}_n) \geq 0$ , and

$$\begin{aligned} &-\min(B(\mathbf{x}_{n+1}), 0) + \min(B(\mathbf{x}_n), 0) \\ &\leq \frac{v_B \rho_3}{1 - \rho_2} [\operatorname{dist}(\mathbf{h}_n, \Omega) - \operatorname{dist}(\mathbf{h}_{n+1}, \Omega)], \end{aligned}$$

for  $B(\mathbf{x}_n) < 0$ , both of which imply (IV.3). Moreover, if  $[\mathbf{x}_n; \mathbf{h}_n] \in \mathcal{C} \times \Omega$ , then, from monotonic approximation property,  $\mathbf{h}_n$  remains in  $\Omega$ , and from (IV.2), the control barrier certificate (III.1) is thus ensured by a control input satisfying (IV.1), rendering the set  $\mathcal{C} \times \Omega$  forward invariant. Therefore, from [62, Theorem 1], the set  $\mathcal{C} \times \Omega$  is asymptotically stable if  $\mathbf{h}_n \notin \Omega_n$  for all  $n \geq N_1$  such that  $[\mathbf{x}_n; \mathbf{h}_n] \notin \mathcal{C} \times \Omega$ .  $\square$

*Remark IV.4* (On Theorem IV.1). Monotonic approximation property plays a key role. If, for example, Bayesian-based learnings such as Gaussian processes are employed for model learning, then it is hard to guarantee any form of monotone approximation after *unexpected and abrupt* change of the agent dynamics in general. This will be analyzed in Section V-A.

For the agent dynamics which keeps changing, the augmented state can be regarded as following a hybrid system, and hence stability should be analyzed under additional assumptions in this case. Such an analysis is beyond the scope of this paper, and we omit the detail.

## B. Structured Model Learning

We have seen that, by employing a model learning with monotone approximation property under Assumption IV.1, the agent is stabilized on the set of safe states even after an abrupt and unexpected change of the agent dynamics. To efficiently enforce control barrier certificates (IV.1), control-affine models are desirable as will be discussed in Section IV-C and Theorem IV.4 therein. Here, we propose a model learning technique that also learns the dynamic structure. We assume that  $n_x = 1$  for simplicity (we can employ  $n_x$  approximators if  $n_x > 1$ ).

First, we show that the space  $\mathcal{H}_c$  (see Section III-C) is an RKHS.

**Lemma IV.1.** The space  $\mathcal{H}_c$  is an RKHS associated with the reproducing kernel  $\kappa(\mathbf{u}, \mathbf{v}) = 1, \forall \mathbf{u}, \mathbf{v} \in \mathcal{U}$ , with the inner product defined as  $\langle \alpha \mathbf{1}, \beta \mathbf{1} \rangle_{\mathcal{H}_c} := \alpha \beta$ ,  $\alpha, \beta \in \mathbb{R}$ .

*Proof.* See Appendix A.  $\square$

Then, the following lemma implies that  $\psi$  can be approximated in the sum space of RKHSs denoted by  $\mathcal{H}_\psi$ .

**Lemma IV.2** ([63, Theorem 13]). Let  $\mathcal{H}_1$  and  $\mathcal{H}_2$  be two RKHSs associated with the reproducing kernels  $\kappa_1$  and  $\kappa_2$ . Then the completion of the tensor product of  $\mathcal{H}_1$  and  $\mathcal{H}_2$ , denoted by  $\mathcal{H}_1 \otimes \mathcal{H}_2$ , is an RKHS associated with the reproducing kernel  $\kappa_1 \otimes \kappa_2$ .

From Lemmas IV.1 and IV.2, we can now assume that  $\hat{f} \in \mathcal{H}_f \otimes \mathcal{H}_c$  and  $\hat{g} \in \mathcal{H}_g \otimes \mathcal{H}_u$ , where  $\hat{g}$  is an estimate of  $\tilde{g}(\mathbf{x}, \mathbf{u}) = g(\mathbf{x})\mathbf{u}$ . As such,  $\psi$  can be approximated in the RKHS  $\mathcal{H}_\psi := \mathcal{H}_p + \mathcal{H}_f \otimes \mathcal{H}_c + \mathcal{H}_g \otimes \mathcal{H}_u$ .

Second, the following theorem ensures that  $\psi$  can be uniquely decomposed into  $p$ ,  $f$ , and  $\tilde{g}$  in the RKHS  $\mathcal{H}_\psi$ .

**Theorem IV.2.** Assume that  $\mathcal{X}$  and  $\mathcal{U}$  have nonempty interiors. Assume also that  $\mathcal{H}_p$  is a Gaussian RKHS. Then,  $\mathcal{H}_\psi$  is the direct sum of  $\mathcal{H}_p$ ,  $\mathcal{H}_f \otimes \mathcal{H}_c$ , and  $\mathcal{H}_g \otimes \mathcal{H}_u$ , i.e., the intersection of any two of the RKHSs  $\mathcal{H}_p$ ,  $\mathcal{H}_f \otimes \mathcal{H}_c$ , and  $\mathcal{H}_g \otimes \mathcal{H}_u$  is  $\{0\}$ .

*Proof.* See Appendix B.  $\square$

*Remark IV.5* (On Theorem IV.2). Because only the control-affine part of the learned model will be used in combination with barrier certificates (see Assumption IV.2 and Theorem IV.4) and the term  $p$  is assumed to be a system noise added to the control-affine dynamics (see Section III-C), the unique decomposition is crucial; if the unique decomposition does not hold, the term  $p$  is able to estimate the overall dynamics, including the control-affine terms.

Therefore, we can employ a multikernel adaptive filter working in the sum space  $\mathcal{H}_\psi$ . By using a sparse optimization for the coefficient vector  $\mathbf{h}_n \in \mathbb{R}^r$ , we wish to extract a structure of the model; The term  $\hat{p}_n$  is desired to be dropped off when the true agent dynamics is control affine.

In order to use the learned model in combination with control barrier functions, each entry of the vector  $\hat{g}_n(\mathbf{x}_n)$  is required. Assume, without loss of generality, that  $\{\mathbf{e}_i\}_{i \in \{1, 2, \dots, n_u\}} \subset \mathcal{U}$  (this is always possible for  $\mathcal{U} \neq \emptyset$  by transforming coordinates of the control inputs and reducing the dimension  $n_u$  if necessary). Then, the  $i$ th entry of the vector  $\hat{g}_n(\mathbf{x}_n)$  is given by  $\hat{g}_n(\mathbf{x}_n)\mathbf{e}_i = \hat{g}_n(\mathbf{x}_n, \mathbf{e}_i)$ . Finally, we can use the learned model effectively to constrain control inputs by control barrier functions for policy updates. Adaptive action-value function approximation with barrier-certified policy updates will be presented in the next subsection.

### C. Adaptive Action-value Function Approximation with Barrier-certified Policy Updates

So far, we showed that an agent can be brought back to safety by employing control barrier certificates and an adaptive model learning with monotone approximation property, and that a control-affine structure can be extracted by employing a sparse adaptive filter working in a certain RKHS. In this subsection, we present an adaptive action-value function approximation with barrier-certified policy updates.

We showed in Section III-D that the Bellman equation in (II.2) is solved via iterative nonlinear function estimation with the input-output pairs  $\{([\mathbf{x}_n; \mathbf{u}_n; \mathbf{x}_{n+1}], \phi(\mathbf{x}_{n+1})), R(\mathbf{x}_n, \mathbf{u}_n)\}_{n \in \mathbb{Z}_{\geq 0}}$ . The following theorem states that the iterative learning can be conducted in an RKHS, and hence any kernel-based method can be employed for action-value function approximation.

**Theorem IV.3.** Suppose that  $\mathcal{H}_Q$  is an RKHS associated with the reproducing kernel  $\kappa^Q(\cdot, \cdot) : \mathcal{Z} \times \mathcal{Z} \rightarrow \mathbb{R}$ . Define, for  $\gamma \in (0, 1)$ ,

$$\mathcal{H}_{\psi^Q} := \{\varphi | \varphi([\mathbf{z}; \mathbf{w}]) = \varphi^Q(\mathbf{z}) - \gamma\varphi^Q(\mathbf{w}), \\ \exists \varphi^Q \in \mathcal{H}_Q, \forall \mathbf{z}, \mathbf{w} \in \mathcal{Z}\}.$$

Then, the operator  $U : \mathcal{H}_Q \rightarrow \mathcal{H}_{\psi^Q}$  defined by  $U(\varphi^Q)([\mathbf{z}; \mathbf{w}]) := \varphi^Q(\mathbf{z}) - \gamma\varphi^Q(\mathbf{w}), \forall \varphi^Q \in \mathcal{H}_Q$ , is bijective.

Moreover,  $\mathcal{H}_{\psi^Q}$  is an RKHS with the inner product defined by

$$\langle \varphi_1, \varphi_2 \rangle_{\mathcal{H}_{\psi^Q}} := \left\langle \varphi_1^Q, \varphi_2^Q \right\rangle_{\mathcal{H}_Q}, \quad (IV.4)$$

$$\varphi_i([\mathbf{z}; \mathbf{w}]) := \varphi_i^Q(\mathbf{z}) - \gamma\varphi_i^Q(\mathbf{w}), \forall \mathbf{z}, \mathbf{w} \in \mathcal{Z}, i \in \{1, 2\}.$$

The reproducing kernel of the RKHS  $\mathcal{H}_{\psi^Q}$  is given by

$$\kappa([\mathbf{z}; \mathbf{w}], [\tilde{\mathbf{z}}; \tilde{\mathbf{w}}]) \\ := (\kappa^Q(\mathbf{z}, \tilde{\mathbf{z}}) - \gamma\kappa^Q(\mathbf{z}, \tilde{\mathbf{w}})) \\ - \gamma(\kappa^Q(\mathbf{w}, \tilde{\mathbf{z}}) - \gamma\kappa^Q(\mathbf{w}, \tilde{\mathbf{w}})), \mathbf{z}, \mathbf{w}, \tilde{\mathbf{z}}, \tilde{\mathbf{w}} \in \mathcal{Z}. \quad (IV.5)$$

*Proof.* See Appendix C.  $\square$

From Theorem IV.3, any kernel-based method can be applied by assuming that  $Q^\phi \in \mathcal{H}_Q$  for a policy  $\phi$ . The estimate of  $Q^\phi$  denoted by  $\hat{Q}^\phi$  is then obtained as  $U^{-1}(\hat{\psi}^Q)$ , where  $\hat{\psi}^Q$  is the estimate of  $\psi^Q \in \mathcal{H}_{\psi^Q}$ . For instance, suppose that the estimate of  $\psi^Q(\mathbf{z}, \mathbf{w})$  for an input  $[\mathbf{z}; \mathbf{w}]$  at time instant  $n$  is given by

$$\hat{\psi}_n^Q([\mathbf{z}; \mathbf{w}]) := \mathbf{h}_n^{Q^\top} \mathbf{k}([\mathbf{z}; \mathbf{w}]),$$

where  $\mathbf{h}_n^Q \in \mathbb{R}^r$  is the model parameter, and  $\mathbf{k}([\mathbf{z}; \mathbf{w}]) := [\kappa([\mathbf{z}; \mathbf{w}], [\tilde{\mathbf{z}}_1; \tilde{\mathbf{w}}_1]); \kappa([\mathbf{z}; \mathbf{w}], [\tilde{\mathbf{z}}_2; \tilde{\mathbf{w}}_2]); \dots; \kappa([\mathbf{z}; \mathbf{w}], [\tilde{\mathbf{z}}_r; \tilde{\mathbf{w}}_r])] \in \mathbb{R}^r$  for  $\{\tilde{\mathbf{z}}_j\}_{j \in \{1, 2, \dots, r\}}, \{\tilde{\mathbf{w}}_j\}_{j \in \{1, 2, \dots, r\}} \subset \mathcal{Z}$  and for  $\kappa(\cdot, \cdot)$  defined by (IV.5). Then, the estimate of  $Q^\phi(\mathbf{z})$  for an input  $\mathbf{z}$  at time instant  $n$  is given by

$$\hat{Q}_n^\phi(\mathbf{z}) := \mathbf{h}_n^{Q^\top} \mathbf{k}^Q(\mathbf{z}), \quad (IV.6)$$

where  $\mathbf{k}^Q(\mathbf{z}) := [U^{-1}(\kappa(\cdot, [\tilde{\mathbf{z}}_1; \tilde{\mathbf{w}}_1]))(\mathbf{z}); \dots; U^{-1}(\kappa(\cdot, [\tilde{\mathbf{z}}_r; \tilde{\mathbf{w}}_r]))(\mathbf{z})] \in \mathbb{R}^r$ .

*Remark IV.6* (On Theorem IV.3). Because the domain of  $\mathcal{H}_{\psi^Q}$  is defined as  $\mathcal{Z} \times \mathcal{Z}$  instead of  $\mathcal{Z}$ , the RKHS  $\mathcal{H}_{\psi^Q}$  does not depend on the agent dynamics, and we can conduct adaptive learning working in the same  $\mathcal{H}_{\psi^Q}$  even after the dynamics changes or the policy is updated. This is especially important when analyzing convergence and/or monotone approximation property of action-value function approximation under possibly nonstationary agent dynamics (see Section V-A.2, for example). As discussed in Appendix G, the Gaussian process SARSA can also be reproduced by applying a Gaussian process in the space  $\mathcal{H}_{\psi^Q}$ , although the Gaussian process SARSA or other kernel-based action-value function approximation is ad-hoc and is designed for learning the action-value function associated with a fixed policy and for a stationary agent dynamics.

When the parameter  $\mathbf{h}_n^Q$  for the estimator  $\hat{\psi}_n^Q$  is monotonically approaching to an optimal point  $\mathbf{h}^{Q^*}$  in the Euclidean norm sense, so is the model parameter for the action-value function because the same parameter is used to estimate  $\psi^Q$  and  $Q^\phi$ . Suppose we employ a method in which  $\hat{\psi}_n^Q$  is monotonically approaching to an optimal function  $\psi^{Q^*}$  in the Hilbertian norm sense. Then, the following corollary implies that an estimator of the action-value function also satisfies the monotonicity.

**Corollary IV.1.** Let  $\mathcal{H}_{\psi^Q} \ni \hat{\psi}_n^Q([\mathbf{z}; \mathbf{w}]) := \hat{Q}_n^\phi(\mathbf{z}) - \gamma\hat{Q}_n^\phi(\mathbf{w})$  and  $\mathcal{H}_{\psi^Q} \ni \psi^{Q^*}([\mathbf{z}; \mathbf{w}]) := Q^{Q^*}(\mathbf{z}) - \gamma Q^{Q^*}(\mathbf{w}), \mathbf{z}, \mathbf{w} \in \mathcal{Z}$ ,

where  $\hat{Q}_n^\phi, Q^{\phi^*} \in \mathcal{H}_Q$ . Then, if  $\hat{\psi}_n^Q$  is approaching to  $\psi^{Q^*}$  in the Hilbertian norm sense, i.e.,

$$\left\| \hat{\psi}_{n+1}^Q - \psi^{Q^*} \right\|_{\mathcal{H}_{\psi^Q}} \leq \left\| \hat{\psi}_n^Q - \psi^{Q^*} \right\|_{\mathcal{H}_{\psi^Q}},$$

it holds that

$$\left\| \hat{Q}_{n+1}^\phi - Q^{\phi^*} \right\|_{\mathcal{H}_Q} \leq \left\| \hat{Q}_n^\phi - Q^{\phi^*} \right\|_{\mathcal{H}_Q}.$$

*Proof.* See Appendix D.  $\square$

Note that employing the action-value function enables us to use random control inputs instead of the target policy  $\phi$  for exploration, and we require no model of the agent dynamics for policy updates as discussed below.

For a current policy  $\phi : \mathcal{X} \rightarrow \mathcal{U}$ , assume that the action-value function  $Q^\phi$  with respect to  $\phi$  at time instant  $n$  is available. Given a discrete-time exponential control barrier function  $B$  and  $0 < \eta \leq 1$ , the barrier certified safe control space is define as

$$\mathcal{S}(\mathbf{x}_n) := \{\mathbf{u}_n \in \mathcal{U} \mid B(\mathbf{x}_{n+1}) - B(\mathbf{x}_n) \geq -\eta B(\mathbf{x}_n)\}.$$

From Proposition III.1, the set  $\mathcal{L}$  defined in (II.4) is forward invariant and asymptotically stable if  $\mathbf{u}_n \in \mathcal{S}(\mathbf{x}_n)$  for all  $n \in \mathbb{Z}_{\geq 0}$ . Then, the updated policy  $\phi^+$  given by

$$\phi^+(\mathbf{x}) := \operatorname{argmax}_{\mathbf{u} \in \mathcal{S}(\mathbf{x})} [Q^\phi(\mathbf{x}, \mathbf{u})], \quad (\text{IV.7})$$

is well-known (e.g., [64], [65]) to satisfy that  $Q^\phi(\mathbf{x}, \phi(\mathbf{x})) \leq Q^{\phi^+}(\mathbf{x}, \phi^+(\mathbf{x}))$ , where  $Q^{\phi^+}$  is the action-value function with respect to  $\phi^+$  at time instant  $n$ . In practice, we use the estimate of  $Q^\phi$  because the exact function  $Q^\phi$  is unavailable. For example, the action-value function is estimated over  $N_f \in \mathbb{Z}_{>0}$  iterations, and the policy is updated every  $N_f$  iterations. To obtain analytical solutions for (IV.7), we follow the arguments in [35]. Suppose that  $\hat{Q}_n^\phi$  is given by (IV.6). We define the reproducing kernel  $\kappa^Q$  of  $\mathcal{H}_Q$  as the tensor kernel given by

$$\kappa^Q([\mathbf{x}; \mathbf{u}], [\mathbf{y}; \mathbf{v}]) := \kappa^x(\mathbf{x}, \mathbf{y}) \kappa^u(\mathbf{u}, \mathbf{v}), \quad (\text{IV.8})$$

where  $\kappa^u(\mathbf{u}, \mathbf{v})$  is, for example, defined by

$$\kappa^u(\mathbf{u}, \mathbf{v}) := 1 + \frac{1}{4} (\mathbf{u}^\top \mathbf{v}).$$

Then, (IV.7) becomes

$$\phi^+(\mathbf{x}) := \operatorname{argmax}_{\mathbf{u} \in \mathcal{S}(\mathbf{x})} \left[ \mathbf{h}_n^{Q^\top} \mathbf{k}^Q([\mathbf{x}; \mathbf{u}]) \right], \quad (\text{IV.9})$$

where the target value being maximized is linear to  $\mathbf{u}$  at  $\mathbf{x}$ . Therefore, if the set  $\mathcal{S}(\mathbf{x}) \subset \mathcal{U}$  is convex, an optimal solution to (IV.9) is guaranteed to be globally optimal, ensuring the greedy improvement of the policy.

As pointed out in [24],  $\mathcal{S}(\mathbf{x}) \subset \mathcal{U}$  is not a convex set in general. To ensure convexity, we consider the set  $\hat{\mathcal{S}}(\mathbf{x}) \subset \mathcal{S}(\mathbf{x}) \subset \mathcal{U}$  under the following moderate assumptions:

- Assumption IV.2.** 1) The set  $\mathcal{U}$  is convex.  
2) Existence of Lipschitz continuous gradient of the barrier function: Given

$$\mathcal{R} := \{(1-t)\mathbf{x}_n + t(\hat{f}_n(\mathbf{x}_n) + \hat{g}_n(\mathbf{x}_n)\mathbf{u}) \mid t \in [0, 1], \mathbf{u} \in \mathcal{U}\},$$

there exists a constant  $v \geq 0$  such that the gradient of the discrete-time exponential control barrier function  $B$ , denoted by  $\frac{\partial B(\mathbf{x})}{\partial \mathbf{x}}$ , satisfies

$$\left\| \frac{\partial B(\mathbf{a})}{\partial \mathbf{x}} - \frac{\partial B(\mathbf{b})}{\partial \mathbf{x}} \right\|_{\mathbb{R}^{n_x}} \leq v \|\mathbf{a} - \mathbf{b}\|_{\mathbb{R}^{n_x}}, \quad \forall \mathbf{a}, \mathbf{b} \in \mathcal{R}.$$

Then, the following theorem holds.

**Theorem IV.4.** Given Assumptions IV.2, IV.1.4, and that  $\|\mathbf{x}_{n+1} - (\hat{f}_n(\mathbf{x}_n) + \hat{g}_n(\mathbf{x}_n)\mathbf{u}_n + \mathbf{x}_n)\|_{\mathbb{R}^{n_x}} \leq \frac{\rho_1}{v_B}$ , (III.1) is satisfied at time instant  $n \in \mathbb{Z}_{\geq 0}$ , if  $\mathbf{u}_n$  satisfies the following:

$$\begin{aligned} & \frac{\partial B(\mathbf{x}_n)}{\partial \mathbf{x}} (\hat{f}_n(\mathbf{x}_n) + \hat{g}_n(\mathbf{x}_n)\mathbf{u}_n) \\ & \geq -\eta B(\mathbf{x}_n) + \frac{v}{2} \|\hat{f}_n(\mathbf{x}_n) + \hat{g}_n(\mathbf{x}_n)\mathbf{u}_n\|_{\mathbb{R}^{n_x}}^2 + \rho_1. \end{aligned} \quad (\text{IV.10})$$

Moreover, (IV.10) defines a convex constraint for  $\mathbf{u}_n$ .

*Proof.* See Appendix E.  $\square$

*Remark IV.7.* When  $\frac{\partial B(\mathbf{x}_n)}{\partial \mathbf{x}} \hat{g}_n(\mathbf{x}_n) \neq 0$  and  $\mathcal{U}$  admits sufficiently large value of each entry of  $\mathbf{u}_n$ , then there always exists a  $\mathbf{u}_n$  that satisfies (IV.10).

Theorem IV.4 essentially implies that, even when the gradient of  $B$  along the shift of  $\mathbf{x}_n$  decreases steeply, (III.1) follows if (IV.10) is satisfied. From Theorem IV.4, the set  $\hat{\mathcal{S}}(\mathbf{x}_n)$ , defined as

$$\begin{aligned} \hat{\mathcal{S}}(\mathbf{x}_n) & := \{\mathbf{u}_n \in \mathcal{U} \mid \frac{\partial B(\mathbf{x}_n)}{\partial \mathbf{x}} (\hat{f}_n(\mathbf{x}_n) + \hat{g}_n(\mathbf{x}_n)\mathbf{u}_n) \\ & \geq -\eta B(\mathbf{x}_n) + \frac{v}{2} \|\hat{f}_n(\mathbf{x}_n) + \hat{g}_n(\mathbf{x}_n)\mathbf{u}_n\|_{\mathbb{R}^{n_x}}^2 + \rho_1\} \subset \mathcal{S}(\mathbf{x}_n), \end{aligned} \quad (\text{IV.11})$$

is convex if  $\mathcal{U} \subset \mathbb{R}^{n_u}$  is convex.

As witnessed in the literatures (e.g., [22]), an agent might encounter deadlock situations, where the constrained control keeps the agent remain in the same state, when control barrier certificates are employed. It is even possible that there is no safe control driving the agent from those states. However, an elaborative design of control barrier functions remedies this issue, as shown in the following example.

**Example IV.1.** If the agent is nonholonomic, turning inward safe regions when approaching their boundary might be infeasible. To reduce the risk of such deadlock situations, control barrier functions may be designed as

$$B(\mathbf{x}) = \tilde{B}(\mathbf{x}) - v\Gamma \left( \left| \theta - \operatorname{atan2} \left\{ \frac{\partial \tilde{B}(\mathbf{x})}{\partial y}, \frac{\partial \tilde{B}(\mathbf{x})}{\partial x} \right\} \right| \right), \quad v > 0,$$

where the state  $\mathbf{x} = [x; y; \theta]$  consists of the X position  $x$ , the Y position  $y$ , and the orientation  $\theta$  of an agent from the world frame,  $\{\mathbf{x} \in \mathcal{X} \mid \tilde{B}(\mathbf{x}) \geq 0\}$  is the original safe region, and  $\Gamma$  is a strictly increasing function. If this control barrier function exists, then the agent is forced to turn inward the original safe region before reaching its boundaries because the control barrier function also depends on  $\theta$  and takes larger value when the agent is facing inward the safe region.

An illustration of Example IV.1 is given in Figure IV.1.

Resulting barrier-certified adaptive reinforcement learning framework is summarized in Algorithm 1.



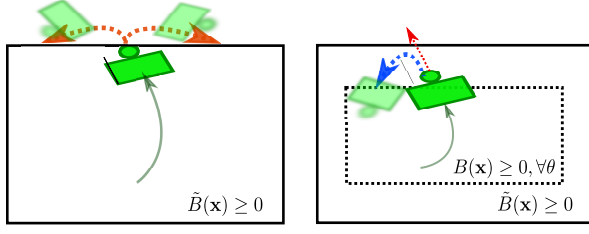


Fig. IV.1. An illustration of how a nonholonomic agent avoids deadlocks. When the orientation of the agent is not considered (i.e.,  $\tilde{B}(\mathbf{x})$  is the barrier function), there might be no safe control driving the agent from those states as the left figure shows. By taking into account the orientation (i.e.,  $B(\mathbf{x})$  is the barrier function), the agent turns inward the safe region before reaching its boundaries as the right figure shows.

---

### Algorithm 1 Barrier-certified adaptive reinforcement learning

---

**Requirement:** Assumptions IV.1 and IV.2; monotone approximation property for model learning;  $\kappa^{\mathcal{Q}}$  defined as (IV.8);  $\mathbf{x}_0 \in \mathcal{X}$  and  $\mathbf{u}_0 \in \mathcal{U}$

**Output:**  $\hat{Q}_n^{\theta}(\mathbf{z}_n)$  ▷ (IV.6)

**for**  $n \in \mathbb{Z}_{\geq 0}$  **do**

- Sample  $\mathbf{x}_n, \mathbf{x}_{n+1} \in \mathcal{X}$ ,  $\mathbf{u}_n \in \mathcal{S}$ , and  $R(\mathbf{x}_n, \mathbf{u}_n) \in \mathbb{R}$
- Obtain  $\phi(\mathbf{x}_{n+1}) \in \hat{\mathcal{S}}_n(\mathbf{x}_{n+1})$  ▷ (IV.11)

**if** Random Exploration **then**

- A (uniformly) random control input  $\mathbf{u}_{n+1} \in \hat{\mathcal{S}}_n(\mathbf{x}_{n+1})$  ▷ (IV.11)

**else**

- $\mathbf{u}_{n+1} = \phi(\mathbf{x}_{n+1})$

**end if**

- Update  $\mathbf{h}_n$  by model learning with monotone approximation property ▷ e.g., Appendix F
- Update  $\mathbf{h}_n^{\mathcal{Q}}$  by a kernel method ▷ Theorem IV.3 and e.g., Appendix F

**if**  $n \bmod N_f = 0$  **then**

- Update  $\phi$ , and let  $\phi = \phi^+$  ▷ (IV.11) and (IV.7)

**end if**

**end for**

---

## V. EXPERIMENTAL RESULTS

For the sake of reproducibility and for clarifying each contribution, we first validate the proposed learning framework on simulations of vertical movements of a quadrotor, which has been used in the safe learnings literature under stationarity assumption (e.g., [7]). Then, we test the proposed learning framework on a real robot called *brushbot*, whose dynamics is unknown, highly complex, and most probably nonstationary<sup>3</sup>. The experiments on the *brushbot* was conducted at the Robotarium, a remotely accessible robot testbed at Georgia institute of technology [66].

### A. Validations of the Safe Learning Framework via Simulations of a Quadrotor

In this experiment, we empirically validate Theorem IV.1 (i.e., Lyapunov stability of the safe set after an unexpected and

<sup>3</sup>Note that the dynamics of a brushbot depends on the body structure, conditions of the brushes, floors, and many other factors, and simulators of the brushbot are thus unavailable.

abrupt change of the agent dynamics) and the motivations of using a online kernel method working in the RKHS  $\mathcal{H}_{\psi^{\mathcal{Q}}}$  (see Section IV-C) for action-value function approximation, and test the proposed framework for simulated vertical movements of a quadrotor. We use parametric model for the agent dynamics and nonparametric model for the action-value function in this experiment. The discrete-time dynamics of the vertical movement of a quadrotor is given by

$$\begin{aligned} \mathbf{x}_{n+1} &= \Xi(\mathbf{z}_n) \mathbf{h}^* := h_1^* \xi_1(\mathbf{z}_n) + h_2^* \xi_2(\mathbf{z}_n) + h_3^* \xi_3(\mathbf{z}_n) \\ &:= h_1 \begin{bmatrix} 1 & \Delta t \\ 0 & 1 \end{bmatrix} \mathbf{x}_n + h_2 \begin{bmatrix} -\frac{\Delta t^2}{2} \\ -\Delta t \end{bmatrix} + h_3 \begin{bmatrix} -\frac{\Delta t^2}{2} \\ -\Delta t \end{bmatrix} \mathbf{u}_n, \\ \mathbf{h}^* &:= [h_1^*; h_2^*; h_3^*] \in \mathbb{R}^3, \xi_i: \mathcal{Z} \rightarrow \mathbb{R}, i \in \{1, 2, 3\}, \\ \mathbf{z}_n &:= [\mathbf{x}_n; \mathbf{u}_n] \in \mathcal{Z}, \mathbf{x}_n := [x_n; \dot{x}_n], \end{aligned}$$

where  $\Delta t \in (0, \infty)$  denotes the time interval,  $x_n$  and  $\dot{x}_n$  are the vertical position and the vertical velocity of the quadrotor at time instant  $n$ , respectively. When the weight of the quadrotor is 0.027kg, the nominal model is given by  $h_1 = 1$ ,  $h_2 = 9.81$ , and  $h_3 = 1/0.027$ . Let the time interval  $\Delta t$  be 0.02 seconds for the simulations, and the maximum input  $2 \times 0.027 \times 9.81$ .

Control barrier certificates are used to limit the region of exploration to the area:  $x \in [-3, 3]$ , and we employ the following two barrier functions:

$$\begin{aligned} B_l(\mathbf{x}) &= 3 - x, \\ B_b(\mathbf{x}) &= x + 3, \end{aligned}$$

and we use the barrier-certificate parameter  $\eta = 0.01$  (see (III.1)) in this experiment. Note that the safe set is equivalently expressed by

$$\mathcal{C} = [-3, 3] = \{\mathbf{x} \in \mathcal{X} | B_l(\mathbf{x}) \geq 0 \wedge B_b(\mathbf{x}) \geq 0\},$$

and the barrier functions satisfy Assumption IV.2.2 with the Lipschitz constant  $v = 0$ .

The immediate reward is given by

$$R(\mathbf{x}, \mathbf{u}) = -2x^2 - \frac{1}{2}\dot{x}^2 + 12, \forall n \in \mathbb{Z}_{\geq 0},$$

where the constant is added to prevent the resulting value of explored states from becoming negative, i.e., lower than the value outside of the safe set.

1) *Stability of the Safe Set:* We compare a Gaussian process (GP) based approach and our proposed framework in terms of safety recovery. Random explorations by uniformly random control inputs are conducted for the first 20 seconds corresponding to 1000 iterations under the dynamics  $\mathbf{h}^* := [1; 9.81; 1/0.027]$ . Then, we change the simulated dynamics and observe if the quadrotor is stabilized on the safe set. To clearly visualize the difference between a GP-based approach and our proposed framework, we let the new agent dynamics be  $\mathbf{h}^* := [1; 9.81; 5/0.027]$ , which is an extreme situation where the maximum input generates very large acceleration.

We define the update rule for adaptive learning as

$$\mathbf{h}_{n+1} = \mathbf{h}_n - \lambda \Xi^{\top}(\mathbf{z}_n) (\Xi(\mathbf{z}_n) \Xi^{\top}(\mathbf{z}_n))^{-1} (\Xi(\mathbf{z}_n) \mathbf{h}_n - \mathbf{x}_{n+1}),$$

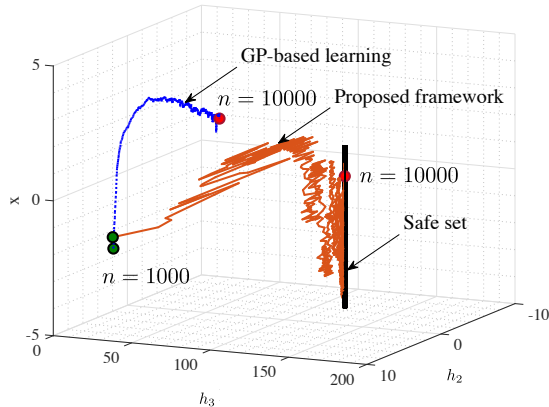


Fig. V.1. Trajectories of the vector  $[x; h_2; h_3]$  of the GP-based learning with barrier certificates and our proposed framework from  $n = 1000$  to  $n = 10000$ . The trajectory of our framework converges to the forward invariant set  $\mathcal{C} \times \Omega$ , while that of GP-based learning does not.

which satisfies the monotone approximation property<sup>4</sup>, where  $\lambda \in (0, 2)$  is the step size. In this experiment, we used  $\lambda = 0.6$ . For the GP-based learning, on the other hand, we let the noise variance of the output be 0.01, and let the prior covariance of the parameter vector  $\mathbf{h}$  be  $25I$ .

The trajectories of the vector  $[x; h_2; h_3]$  of the GP-based learning with barrier certificates and our proposed framework from  $n = 1000$  to  $n = 10000$  are plotted in Figure V.1. We can observe that the trajectory of our framework converges to the forward invariant set  $\mathcal{C} \times \Omega$ , while that of GP-based learning does not.

2) *Adaptive Action-value Function Approximation:* We also compare a GP-based reinforcement learning (the GP SARSA), and a kernel adaptive filter for action-value function approximation. The parameter settings for the kernel adaptive filter are summarized in Table V.1. Please refer to Appendix F for the notations which are not in the main text. Six Gaussian kernels with different scale parameters  $\sigma$  are employed for the kernel adaptive filter (i.e.,  $M = 6$ . See also Appendix F for more detail about multikernel adaptive filter). For the GP SARSA, we employ a Gaussian kernel with scale parameter 3, which achieved sufficiently good performance, and let the noise variance of the output be  $10^{-6}$  (i.e.,  $\Sigma = 10^{-6}I$ . See Appendix G.). Other parameters are the same as those of the kernel adaptive filter. In addition, we also test the GP SARSA in another settings, where the kernel function is added in the first 600 iterations (i.e., dimension of the parameter becomes  $r = 600$ ) and is not newly added after 600 iterations. We call this as the GP SARSA 2 for convenience in this section. We employ an adaptive model learning for all of the three reinforcement learning approaches, and update policies every 1000 iterations. For the comparison purpose, we do not reset learning even when the policy is updated.

<sup>4</sup>This update is viewed as a projection of the current parameter onto the affine set any of whose element  $\mathbf{h}_n^*$  satisfies  $\Xi(\mathbf{z}_n)\mathbf{h}_n^* - \mathbf{x}_{n+1} = 0$ , and hence it follows that  $\|\mathbf{h}_{n+1} - \mathbf{h}_n^*\|_{\mathbb{R}^3} < \|\mathbf{h}_n - \mathbf{h}_n^*\|_{\mathbb{R}^3}$ ,  $\forall \mathbf{h}_n^* \in \Omega_n := \arg\min_{\mathbf{h} \in \mathbb{R}^r} [\Xi(\mathbf{z}_n)\mathbf{h} - \mathbf{x}_{n+1}]$ .

TABLE V.1

SUMMARY OF THE PARAMETER SETTINGS OF THE SIMULATED VERTICAL MOVEMENTS OF A QUADROTOR (KERNEL ADAPTIVE FILTER)

Parameter	Description	Values
$\lambda$	step size	0.1
$s$	data size	5
$\mu$	regularization parameter	0.01
$\varepsilon_1$	precision parameter	0.2
$\varepsilon_2$	large-normalized-error	0.1
$r_{\max}$	maximum-dictionary-size	600
$\sigma$	scale parameters	{50, 30, 10, 5, 2, 1}
$\gamma$	discount factor	0.9

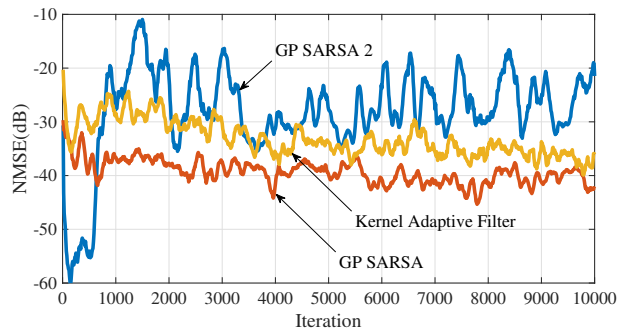


Fig. V.2. The learning curves of the normalized mean squared errors (NMSEs) of action-value function approximation for the GP SARSA, kernel adaptive filter, and the GP SARSA 2.

Random explorations by uniformly random control inputs are conducted for the first 200 seconds corresponding to 10000 iterations under the dynamics  $\mathbf{h}^* := [1; 9.81; 1/0.027]$ , and the dynamics changes to  $\mathbf{h}^* := [1; 11.81; 0.9/0.027]$  (i.e., additional downward accelerations and degradations of batteries, for example) at time instant  $n = 2500$ . We evaluate the policy obtained at time instant  $n = 10000$  for five times with different initial states, and we also conduct 15 runs for learning. For each policy evaluation, the initial state follows the uniform distribution for the position  $\mathbf{x}$  with the velocity  $\dot{\mathbf{x}} = 0$ .

The learning curves of the normalized mean squared errors (NMSEs) of action-value function approximation, which are averaged over 15 runs and smoothed, for the GP SARSA, the kernel adaptive filter, and the GP SARSA 2, are plotted in Figure V.2. From Figure V.2, we can observe that both the GP SARSA and the kernel adaptive filter show no large degradations of the NMSE even after the dynamics changes or the policy is updated, while the GP SARSA 2 stops improving the NMSE after the policy is updated (and the dynamics is changed). Because no kernel function is newly added after the first 600 iterations, the GP SARSA 2 could not adapt to the new policy or new dynamics.

The expected values  $E[V^\phi(\mathbf{x})]$  (expectation is taken over the  $15 \times 5$  runs, i.e., 15 runs for learning, each of which includes five policy evaluations) associated with the policies obtained at time instant  $n = 10000$  for the GP SARSA, the kernel adaptive filter, and the GP SARSA 2 are shown in Table V.2. Recall that  $V^\phi$  is defined in (II.1).

Among the 15 runs for the kernel adaptive filter, we extracted the seventh run, which was successful. The left

TABLE V.2

THE EXPECTED VALUES OF THE GP SARSA AND THE KERNEL ADAPTIVE FILTER

GP SARSA	kernel adaptive filter	GP SARSA 2
65.77 ± 41.42	64.68 ± 40.39	63.01 ± 42.50

figure of Figure V.3 illustrates the action-value function at time instant  $n = 10000$  of the seventh run for the kernel adaptive filter, and the right figure of Figure V.3 plots the trajectory of the optimal policy obtained at time instant  $n = 10000$  for the seventh run. The simulated quadrotor was relocated at time instant  $n = 11000, 12000, 13000$ , and  $n = 14000$ , and both the position and the velocity of the simulated quadrotor went to zeros successfully.

3) *Discussion*: The control barrier certificates with adaptive model learning recovered safety even for an extreme situation where the control inputs start generating very large acceleration. As long as model learning satisfies monotone approximation property and Assumption IV.1, safety recovery is guaranteed without having to elaborately tune hyperparameters.

Reinforcement learning with the GP SARSA and kernel adaptive filter in the RKHS  $\mathcal{H}_{\Psi Q}$  worked sufficiently well. If no kernel functions are newly added, GP-based learnings cannot adapt to the new policies or agent dynamics. Therefore, we need to sequentially add new kernel functions or use a sparse adaptive filter to prune redundant kernel functions (see also Appendix F for a sparse adaptive filter).

Our safe learning framework validated by these simulations is now ready to be applied to a real robot called brushbot as presented below.

### B. Real-Robotics Experiments on a Brushbot

Next, we apply our safe learning framework, which was validated by simulations, to a *brushbot*, which has highly nonlinear, nonholonomic, and most probably nonstationary dynamics (see Figure V.4). The objective of this experiment is to find a policy driving the brushbot to the origin, while restricting the region of exploration. The experiment is conducted at the Robotarium, a remotely accessible robot testbed at Georgia institute of technology [66].

1) *Experimental Condition*: The experimental conditions for model learning, reinforcement learning, control barrier functions, and their parameter settings are presented below.

a) *Model learning*: The state  $\mathbf{x} = [x; y; \theta]$  consists of the X position  $x$ , Y position  $y$ , and the orientation  $\theta \in [-\pi, \pi]$  of the brushbot from the world frame. The exact positions and the orientation are recorded by motion capture systems every 0.3 seconds. A control input  $\mathbf{u}$  is of two dimensions each of which corresponds to the rotational speed of a motor. To improve the learning efficiency and reduce the total learning time required, we identify the most significant dimension and reduce the dimensions to learn. The sole input variable of  $p, f$ , and  $g$ , for the shifts of  $x$  and  $y$ , is assumed to be  $\theta$ , and the shift of  $\theta$  is assumed to be constant over the state, and hence depends on nothing but control inputs (see Section V-B.1.d). The brushbot used in the present study is nonholonomic, i.e., it

can only go forward, and positive control inputs basically drive the brushbot in the same way as negative control inputs. As such, we use the rotational speeds of the motors as the control inputs. Moreover, to eliminate the effect of static frictions on the model, we assume that the zero control input given to the algorithm actually generates some minimum control inputs  $u_\delta$  to the motors, i.e., the actual maximum control inputs to the motors are given by  $u_{\max} + u_\delta$ , where  $u_{\max}$  is the maximum control input fed to the algorithm.

b) *Reinforcement learning*: The state for action-value function approximation consists of the distance  $\|[x; y]\|_{\mathbb{R}^2}$  from the origin and the orientation  $\theta - \text{atan2}(y, x)$  which is wrapped to the interval  $[-\pi, \pi]$ . The immediate reward is given by

$$R(\mathbf{x}, \mathbf{u}) = -\|[x; y]\|_{\mathbb{R}^2}^2 + 2, \forall n \in \mathbb{Z}_{\geq 0},$$

where the constant is added to prevent the resulting value of explored states from becoming negative, i.e., lower than the value outside of the region of exploration.

c) *Discrete-time control barrier certificates*: Control barrier certificates are used to limit the region of exploration to the rectangular area:  $x \in [-x_{\max}, x_{\max}]$ ,  $y \in [-y_{\max}, y_{\max}]$ , where  $x_{\max} > 0$  and  $y_{\max} > 0$ . Because the brushbot can only go forward, we employ the following four barrier functions:

$$\begin{aligned} B_1(\mathbf{x}) &= x_{\max} - x - v |\theta + \pi|, \\ B_2(\mathbf{x}) &= x + x_{\max} - v |\theta|, \\ B_3(\mathbf{x}) &= y_{\max} - y - v \left| \theta + \frac{\pi}{2} \right|, \\ B_4(\mathbf{x}) &= y + y_{\max} - v \left| \theta - \frac{\pi}{2} \right|, \end{aligned}$$

(see Example IV.1 for the motivations of using the above control barrier functions). Note that those functions satisfy Assumption IV.2.2 and the Lipschitz constant  $v$  is zero except at around  $\theta = -\frac{\pi}{2}, 0, \frac{\pi}{2}, \pi$ . (Although we can employ globally Lipschitz functions for more rigorous treatment, we use the above functions for simplicity.)

d) *Parameter settings*: The parameter settings are summarized in Table V.3. Please refer to Appendix F for the notations which are not in the main text. Five Gaussian kernels with different scale parameters  $\sigma$  are employed in action-value function approximation (i.e.,  $M = 5$ . See also Appendix F for more detail about multikernel adaptive filter), and six Gaussian kernels are employed in model learning for  $x$  and  $y$  (i.e.,  $M = 6$ ). In model learning for  $\theta$ , we define  $\mathcal{H}_p, \mathcal{H}_f$ , and  $\mathcal{H}_g$  as sets of constant functions.

The kernels of  $\mathcal{H}_p$  and  $\mathcal{H}_f$  are weighed by  $\tau = 0.1$  in model learning (see Lemma F.1 in Appendix F).

e) *Procedure*: The time interval (duration of one iteration) for learning is 0.3 seconds, and random explorations are conducted for the first 300 seconds corresponding to 1000 iterations. While exploring, the model learning algorithm adaptively learns a model whose control-affine terms, i.e.,  $\hat{f}_n(\mathbf{x}) + \hat{g}_n(\mathbf{x})\mathbf{u}$ , is used in combination with barrier certificates. Although barrier functions employed in the experiment reduce deadlock situations, the brushbot is forced to turn inward the region of exploration when a deadlock is detected. Note that the barrier certificates are intentionally violated in such a case. The policy is updated every 50 seconds. After 300 seconds, we

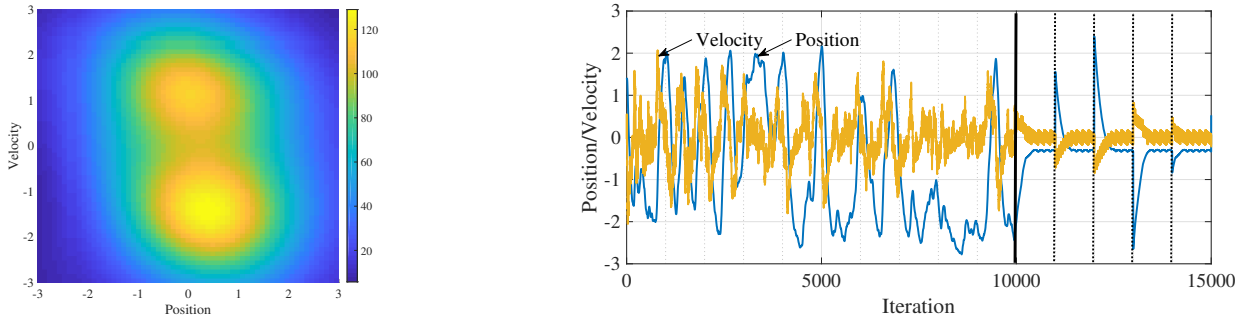


Fig. V.3. The left figure illustrates the action-value function over the position  $x$  and the velocity  $\dot{x}$  at  $n = 10000$  and at the control input  $-0.027 \times 11.81/0.9$ , which cancels out the acceleration added to the quadrotor. Positive velocities for negative positions and negative velocities for positive positions have higher values. The right figure shows the trajectory of the optimal policy obtained at time instant  $n = 10000$  for the seventh run, which was a successful run among the 15 runs. Dashed lines indicate the time when the quadrotor was relocated. Both the position and the velocity of the simulated quadrotor went to zeros successfully.

TABLE V.3  
SUMMARY OF THE PARAMETER SETTINGS

Parameter	Description	General settings		
$x_{\max}$	maximum X position	1.2		
$y_{\max}$	maximum Y position	1.2		
$\eta$	barrier-function parameter	0.1		
$v$	coefficient in barrier functions	0.1		
$u_{\delta}$	actual minimum control	0.4		
$u_{\max}$	maximum control input	0.623		
Parameter	Description	Model Learning (x and y)	Model Learning ( $\theta$ )	Action-value function approximation
$\lambda$	step size	0.3	0.03	0.3
$s$	data size	5	10	10
$\mu$	regularization parameter	0.0001	0	0.0001
$\epsilon_1$	precision parameter	0.001	0.01	0.05
$\epsilon_2$	large-normalized-error	0.1	0.1	0.1
$r_{\max}$	maximum-dictionary-size	500	3	2000
$\sigma$	scale parameters	{10, 5, 2, 1, 0.5, 0.2}	–	{10, 5, 2, 1, 0.5}
$\gamma$	discount factor	–	–	0.95

stop learning a model and the action-value function, and the policy replaces random explorations. The brushbot is forced to stop when it enters into the circle of radius 0.2 centered at the origin. When the brushbot is driven close to the origin and enters this circle, it is pushed away from the origin to see if it returns to the origin again (see Figure V.10).

2) *Results:* Figure V.5 plots  $\hat{p}_n([\mathbf{x}; 0; 0])$ ,  $\hat{f}_n(\mathbf{x})$ ,  $\hat{g}_n^{(1)}(\mathbf{x})$ , and  $\hat{g}_n^{(2)}(\mathbf{x})$  for  $x$  and  $y$  at  $n = 1000$ . Here  $\hat{g}_n^{(i)}$  is the estimate of  $g^{(i)}$  at time instant  $n$ . Recall that these functions only depend on  $\theta$  in this experiment to improve the learning efficiency. For the shift of  $\theta$ , the estimators are constant over the state, and the result is  $\hat{g}_n^{(1)}(\mathbf{x}) = 1.38$ ,  $\hat{g}_n^{(2)}(\mathbf{x}) = -0.77$ , and  $\hat{p}_n([\mathbf{x}; 0; 0]) = \hat{f}_n(\mathbf{x}) = 0$  at  $n = 1000$ . As can be seen in Figure V.5,  $\hat{p}_n([\mathbf{x}; 0; 0])$  is almost zero and so is  $\hat{f}_n(\mathbf{x})$ , implying that the proposed algorithm successfully dropped off irrelevant structural components of a model.

Figure V.6 plots the trajectory of the brushbot while exploring (i.e., X,Y positions from  $n = 0$  to  $n = 1000$ ). It is observed that the brushbot remained in the region of exploration ( $x \in [-1.2, 1.2]$  and  $y \in [-1.2, 1.2]$ ) most of the time. Moreover, the values of barrier functions  $B_i$ ,  $i \in \{1, 2, 3, 4\}$ , for the whole trajectory are plotted in Figure V.7. Even though some violations of safety are seen in the figure, the brushbot returned to the safe region before large violations occurred. Despite unknown, highly complex and possibly nonstationary system,

the proposed safe learning framework was shown to work efficiently.

Figure V.8 plots the trajectories of the optimal policy learned by the brushbot. Once the optimal policy replaced random explorations, the brushbot returned to the origin until  $n = 1016$  as the first figure shows. The brushbot was pushed by a sweeper at time instant  $n = 1031, 1075, 1101, 1128, 1181$ , and  $n = 1230$ , and the trajectories of the brushbot after being pushed at  $n = 1031, 1075, 1101$  are also shown in Figure V.8. Dashed lines in the last figure indicate the time when the brushbot is pushed away. Given relatively short learning time and that no simulator was used, the brushbot learned the desirable behavior sufficiently well.

Figure V.9 plots the shape of  $\hat{Q}_n^\phi(\|\|[\mathbf{x}; \mathbf{y}]\|_{\mathbb{R}^2}; 0, [0; 0])$  over X,Y positions at  $n = 1000$ . It is observed that when the control input is zero (i.e., when the brushbot basically does not move), the vicinity of the origin has the highest value, which is reasonable.

Finally, Figure V.10 shows two trajectories of the brushbot returning to the origin by using the action-value function saved at  $n = 1000$ . After being pushed away from the origin, the brushbot successfully returned to the origin again.

3) *Discussion:* One of the challenges of the experiments is that no initial data or simulators were available. Despite the fact that the brushbot with highly complex system had to learn an optimal policy while dealing with safety by employing

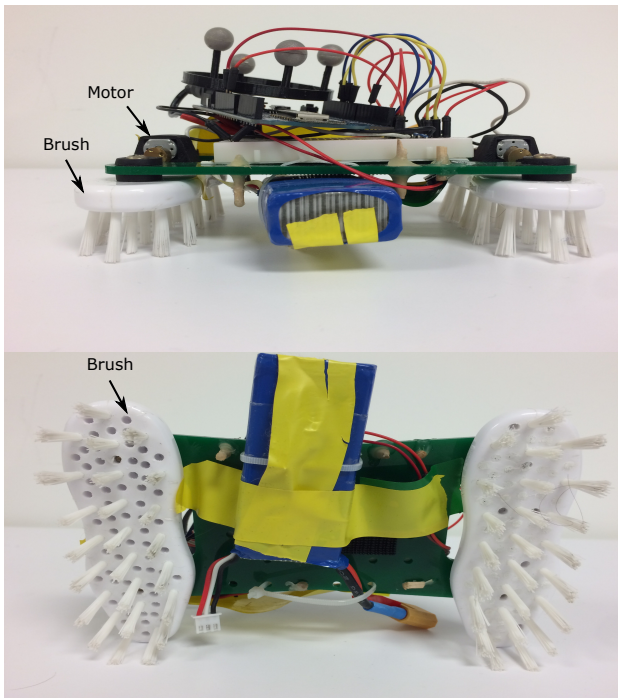


Fig. V.4. A picture of the brushbot used in the experiment. Vibrations of the two motors propagate to the two brushes, driving the brushbot. Control inputs are of two dimensions each of which corresponds to the rotational speed of a motor.

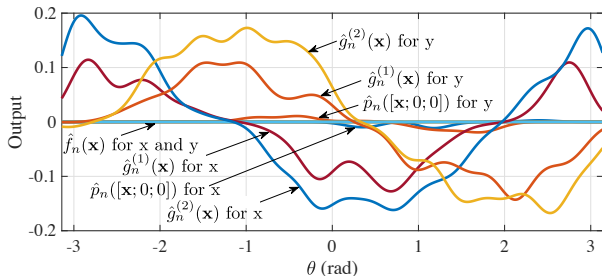


Fig. V.5. Estimated output of the model estimator at  $\mathbf{u} = [0; 0]$  and  $n = 1000$  over the orientation  $\theta$ . Irrelevant structures such as  $\hat{p}_n$  and  $\hat{f}_n$  dropped off successfully.

adaptive model learning, the proposed learning framework worked well in the real world. Brushbot is powered by brushes, and its dynamics highly depends on the conditions of the floor and brushes. The possible changes of the agent dynamics thus lead to some violations of safety. Nevertheless, our learning framework recovered safety quickly. In addition, the agent learned a *good* policy within a quite short period. One reason of those successes of adaptivity and data-efficiency is the convex-analytic formulations.

On the other hand, since our framework is fully adaptive, i.e., we do *not* collect data and conduct batch model learning and/or reinforcement learning, and no initial nominal model or a policy is available. Therefore, we need to reduce the dimensions of input vectors to speed-up and robustify learning. This can be an inherent limitation of our framework.

## VI. CONCLUSION

The learning framework presented in this paper successfully tied model learning, reinforcement learning, and barrier certificates, enabling barrier-certified reinforcement learning for unknown, highly nonlinear, nonholonomic, and possibly nonstationary agent dynamics. The proposed model learning algorithm captures a structure of the agent dynamics by employing a sparse optimization. The resulting model has preferable structure for preserving efficient computations of barrier certificates. In addition, recovery of safety after an unexpected and abrupt change of the agent dynamics was guaranteed by model learning with monotone approximation and barrier certificates under certain conditions. For possibly nonstationary agent dynamics, the action-value function approximation problem was appropriately reformulated so that kernel-based methods, including kernel adaptive filter, can be directly applied. Lastly, certain conditions were also presented to render the set of safe policies convex, thereby guaranteeing the global optimality of solutions to the policy update to ensure the greedy improvement of a policy. The experimental result shows the efficacy of the proposed learning framework in the real world.

### APPENDIX A

#### PROOF OF LEMMA IV.1

Since  $\kappa(\mathbf{u}, \mathbf{v}) = \mathbf{1}(\mathbf{u}) = 1, \forall \mathbf{u}, \mathbf{v} \in \mathcal{U}$ , is a positive definite kernel, it defines the unique RKHS given by  $\text{span}\{\mathbf{1}\}$ , which is complete because it is a finite-dimensional space. For any  $\varphi := \alpha \mathbf{1} \in \mathcal{H}_c$ ,  $\langle \varphi, \varphi \rangle_{\mathcal{H}_c} = \alpha^2 \geq 0$  and the equality holds if and only if  $\alpha = 0$ , or equivalently,  $\varphi = 0$ . The symmetry and the linearity also hold, and hence  $\langle \cdot, \cdot \rangle_{\mathcal{H}_c}$  defines the inner product. For any  $\mathbf{u} \in \mathcal{U}$ , it holds that  $\langle \varphi, \kappa(\cdot, \mathbf{u}) \rangle_{\mathcal{H}_c} = \langle \alpha \mathbf{1}, \mathbf{1} \rangle_{\mathcal{H}_c} = \alpha = \varphi(\mathbf{u})$ . Therefore, the reproducing property is satisfied.

### APPENDIX B

#### PROOF OF THEOREM IV.2

The following lemmas are used to prove the theorem.

**Lemma B.1** ([67, Theorem 2]). Let  $\mathcal{X} \subset \mathbb{R}^{n_x}$  be any set with nonempty interior. Then, the RKHS associated with the Gaussian kernel for an arbitrary scale parameter  $\sigma > 0$  does not contain any polynomial on  $\mathcal{X}$ , including the nonzero constant function.

**Lemma B.2.** Assume that  $\mathcal{X} \subset \mathbb{R}^{n_x}$  and  $\mathcal{U} \subset \mathbb{R}^{n_u}$  have nonempty interiors. Then, the intersection of the RKHS  $\mathcal{H}_u$  associated with the kernel  $\kappa(\mathbf{u}, \mathbf{v}) := \mathbf{u}^\top \mathbf{v}$ ,  $\mathbf{u}, \mathbf{v} \in \mathcal{U}$ , and the RKHS  $\mathcal{H}_c$  is  $\{0\}$ , i.e.,

$$\mathcal{H}_c \cap \mathcal{H}_u = \{0\}.$$

*Proof.* It is obvious that the function  $\varphi(\mathbf{u}) = 0, \forall \mathbf{u} \in \mathcal{U}$ , is an element of both of the RKHSs (vector spaces)  $\mathcal{H}_u$  and  $\mathcal{H}_c$ . Therefore, it is sufficient to show that there exists  $\mathbf{u} \in \mathcal{U}$  satisfying that  $\varphi(\mathbf{u}) \neq \varphi(\mathbf{u}^{\text{int}})$ ,  $\mathbf{u}^{\text{int}} \in \text{int}(\mathcal{U})$ , where  $\text{int}(\mathcal{U})$  denotes the interior of  $\mathcal{U}$ , for any  $\varphi \in \mathcal{H}_u \setminus \{0\}$ . Assume that  $\varphi(\mathbf{v}) \neq 0$  for some  $\mathbf{v} \in \mathcal{U}$ . From [63, Theorem 3], the RKHS  $\mathcal{H}_u$  is expressed as  $\mathcal{H}_u = \text{span}\{\kappa(\cdot, \mathbf{u})\}_{\mathbf{u} \in \mathcal{U}}$ , which is finite dimension, implying that any function in  $\mathcal{H}_u$  is linear. Since

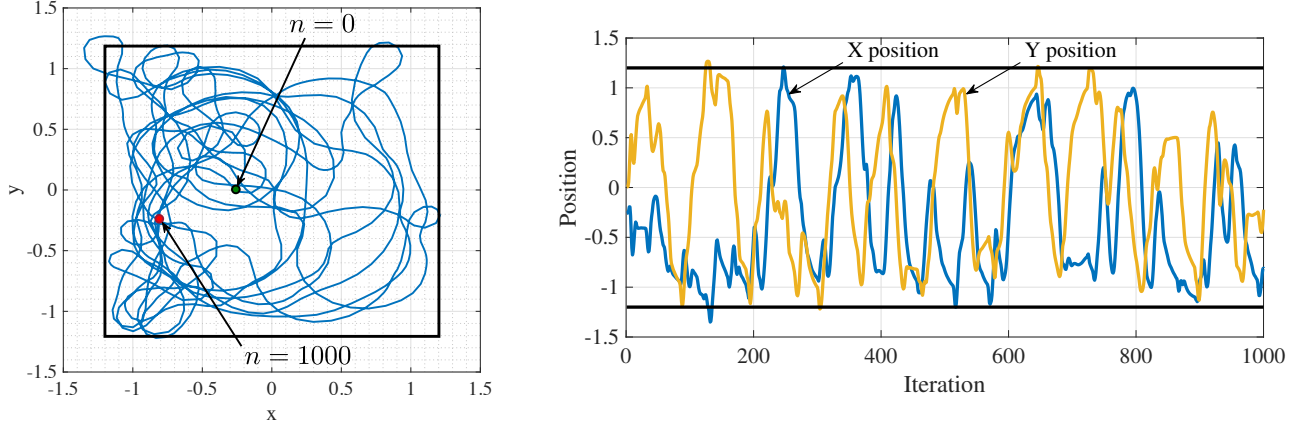


Fig. V.6. The left figure shows the trajectory of the brushbot while exploring, and the right figure shows X,Y positions over iterations. The region of exploration is limited to  $x \in [-1.2, 1.2]$  and  $y \in [-1.2, 1.2]$ . The brushbot remained in the region most of the time.

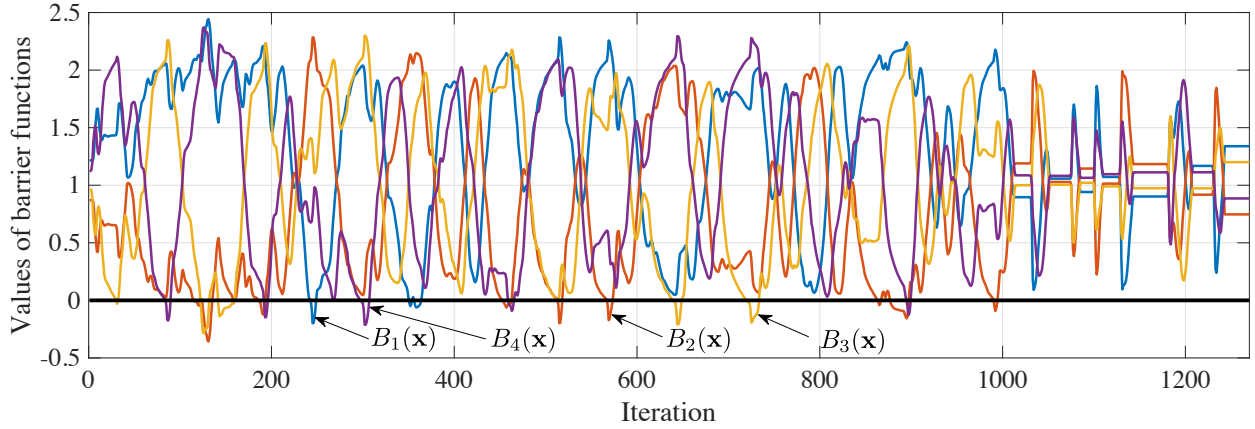


Fig. V.7. The values of four control barrier functions employed in the experiment for the whole trajectory. Even though some violations of safety were seen, the brushbot returned to the safe region before large violations occurred. The nonholonomic brushbot adaptively learned a model and how to turn inward the region of exploration before reaching the boundaries of the region of exploration.

there exists  $\mathbf{u} = \mathbf{u}^{\text{int}} + \rho_4 \mathbf{v} \in \mathcal{U}$  for some  $\rho_4 > 0$ , it is proved that

$$\varphi(\mathbf{u}) = \varphi(\mathbf{u}^{\text{int}} + \rho_4 \mathbf{v}) = \varphi(\mathbf{u}^{\text{int}}) + \rho_4 \varphi(\mathbf{v}) \neq \varphi(\mathbf{u}^{\text{int}}).$$

□

**Lemma B.3** ([68, Proposition 1.3]). If  $\mathcal{H}_2 = \mathcal{H}_{21} \oplus \mathcal{H}_{22}$  for given vector spaces  $\mathcal{H}_1$  and  $\mathcal{H}_2$ , then

$$\mathcal{H}_1 \otimes \mathcal{H}_{21} \cap \mathcal{H}_1 \otimes \mathcal{H}_{22} = \{0\},$$

i.e.,

$$\mathcal{H}_1 \otimes \mathcal{H}_2 = (\mathcal{H}_1 \otimes \mathcal{H}_{21}) \oplus (\mathcal{H}_1 \otimes \mathcal{H}_{22}).$$

**Lemma B.4.** Given  $\mathcal{X} \subset \mathbb{R}^{n_x}$  and  $\mathcal{U} \subset \mathbb{R}^{n_u}$ , let  $\mathcal{H}_1$ ,  $\mathcal{H}_2$ , and  $\mathcal{H}$  be associated with the Gaussian kernels  $\kappa_1(\mathbf{x}, \mathbf{y}) := \frac{1}{(\sqrt{2\pi}\sigma)^{n_x}} \exp\left(-\frac{\|\mathbf{x}-\mathbf{y}\|_{\mathbb{R}^{n_x}}^2}{2\sigma^2}\right)$ ,  $\mathbf{x}, \mathbf{y} \in \mathcal{X}$ ,  $\kappa_2(\mathbf{u}, \mathbf{v}) := \frac{1}{(\sqrt{2\pi}\sigma)^{n_u}} \exp\left(-\frac{\|\mathbf{u}-\mathbf{v}\|_{\mathbb{R}^{n_u}}^2}{2\sigma^2}\right)$ ,  $\mathbf{u}, \mathbf{v} \in \mathcal{U}$ , and  $\kappa([\mathbf{x}; \mathbf{u}], [\mathbf{y}; \mathbf{v}]) := \frac{1}{(\sqrt{2\pi}\sigma)^{n_x+n_u}} \exp\left(-\frac{\|[\mathbf{x}; \mathbf{u}] - [\mathbf{y}; \mathbf{v}]\|_{\mathbb{R}^{n_x+n_u}}^2}{2\sigma^2}\right)$ ,  $\mathbf{x}, \mathbf{y} \in \mathcal{X}$ ,  $\mathbf{u}, \mathbf{v} \in \mathcal{U}$ , respectively, for an arbitrary  $\sigma > 0$ . Then, by regarding a

function in  $\mathcal{H}_1 \otimes \mathcal{H}_2$  as a function over the input space  $\mathcal{X} \times \mathcal{U} \subset \mathbb{R}^{n_x+n_u}$ , it holds that

$$\mathcal{H} = \mathcal{H}_1 \otimes \mathcal{H}_2.$$

*Proof.*  $\mathcal{H}_1 \otimes \mathcal{H}_2$  has the reproducing kernel defined by

$$\begin{aligned} \kappa_{\otimes}([\mathbf{x}; \mathbf{u}], [\mathbf{y}; \mathbf{v}]) &:= \kappa_1(\mathbf{x}, \mathbf{y}) \kappa_2(\mathbf{u}, \mathbf{v}) \\ &= \frac{1}{(\sqrt{2\pi}\sigma)^{n_x} (\sqrt{2\pi}\sigma)^{n_u}} \\ &\exp\left(-\frac{\|\mathbf{x}-\mathbf{y}\|_{\mathbb{R}^{n_x}}^2}{2\sigma^2}\right) \exp\left(-\frac{\|\mathbf{u}-\mathbf{v}\|_{\mathbb{R}^{n_u}}^2}{2\sigma^2}\right) \\ &= \frac{1}{(\sqrt{2\pi}\sigma)^{n_x+n_u}} \exp\left(-\frac{\|\mathbf{x}-\mathbf{y}\|_{\mathbb{R}^{n_x}}^2 + \|\mathbf{u}-\mathbf{v}\|_{\mathbb{R}^{n_u}}^2}{2\sigma^2}\right) \\ &= \kappa([\mathbf{x}; \mathbf{u}], [\mathbf{y}; \mathbf{v}]). \end{aligned}$$

This verifies the claim. □

We are now ready to prove Theorem IV.2.

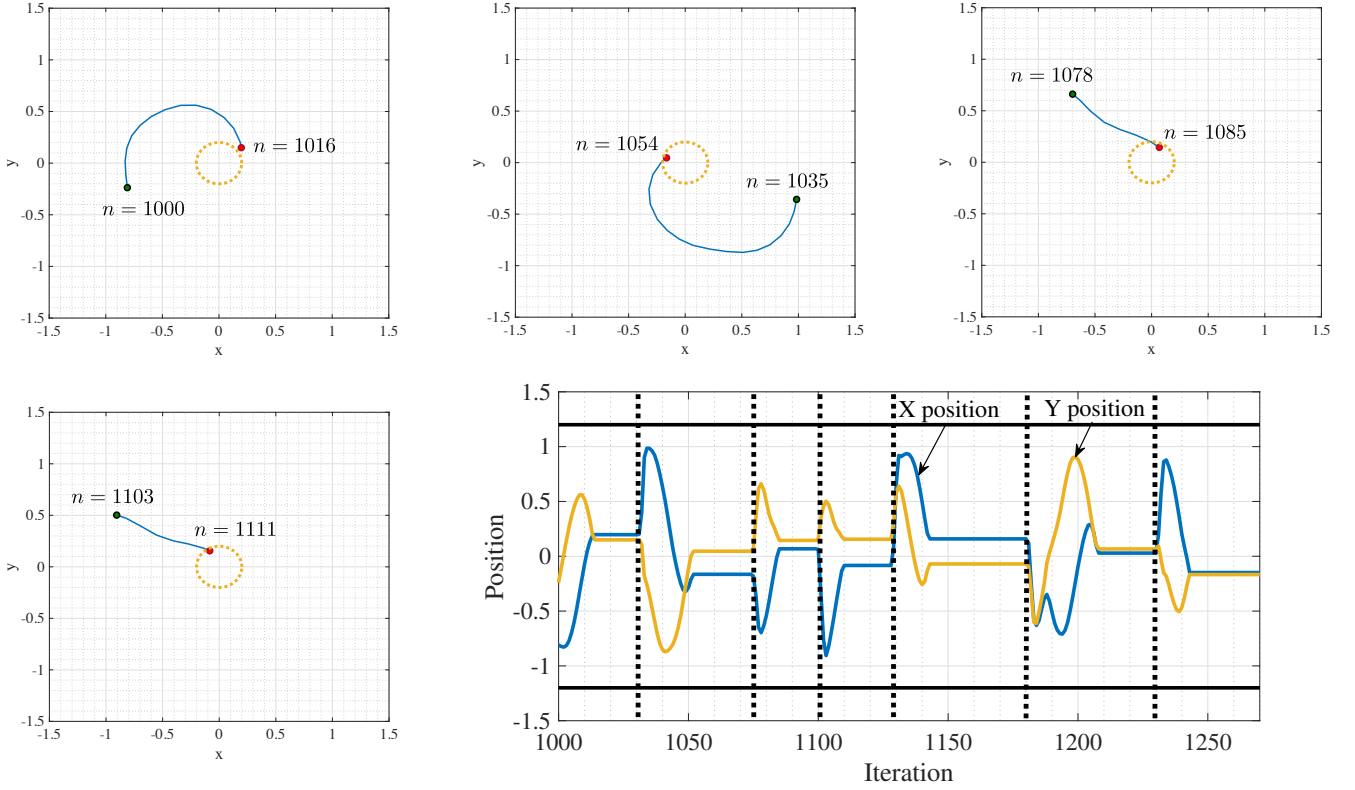


Fig. V.8. Trajectories of the optimal policy learned by the brushbot. The optimal policy replaced random explorations at  $n = 1000$ , and the brushbot returned to the origin until  $n = 1016$  (first figure). The brushbot was pushed by a sweeper at time instant  $n = 1031, 1075, 1101, 1128, 1181$ , and  $n = 1230$ . Dashed lines in the last figure indicate the time when the brushbot was pushed away. The brushbot learned the desirable behavior sufficiently well.

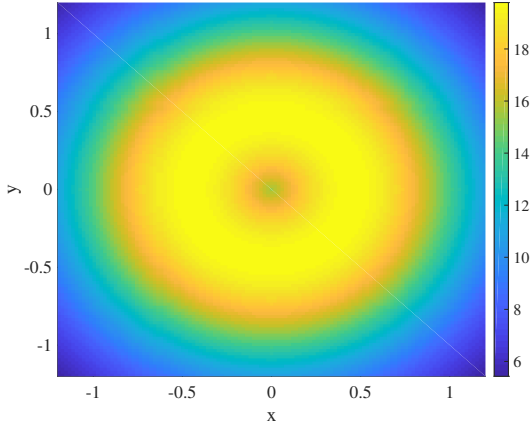


Fig. V.9. The shape of the action-value function over X,Y positions at the control input  $\mathbf{u} = [0; 0]$  and  $n = 1000$ . The vicinity of the origin has the highest value when the control input is zero.

*Proof of Theorem IV.2.* By Lemmas B.2 and B.3, it is derived that  $\mathcal{H}_f \otimes \mathcal{H}_c \cap \mathcal{H}_g \otimes \mathcal{H}_u = \{0\}$ . By Lemmas B.1, B.3, and B.4, it holds that  $\mathcal{H}_p \cap \mathcal{H}_f \otimes \mathcal{H}_c = \{0\}$  and  $\mathcal{H}_p \cap \mathcal{H}_g \otimes \mathcal{H}_u = \{0\}$ .  $\square$

## APPENDIX C PROOF OF THEOREM IV.3

We show that the operator  $U : \mathcal{H}_Q \rightarrow \mathcal{H}_{\Psi^Q}$ , which maps  $\varphi^Q \in \mathcal{H}_Q$  to a function  $\varphi \in \mathcal{H}_{\Psi^Q}$ ,  $\varphi([\mathbf{z}; \mathbf{w}]) = \varphi^Q(\mathbf{z}) - \gamma\varphi^Q(\mathbf{w})$  where  $\gamma \in (0, 1)$ ,  $\mathbf{z}, \mathbf{w} \in \mathcal{Z}$ , is bijective. Because the mapping  $U$  is surjective by definition, we show it is also injective. For any  $\varphi_1^Q, \varphi_2^Q \in \mathcal{H}_Q$ ,

$$\begin{aligned} U(\varphi_1^Q + \varphi_2^Q)([\mathbf{z}; \mathbf{w}]) &= (\varphi_1^Q + \varphi_2^Q)(\mathbf{z}) - \gamma(\varphi_1^Q + \varphi_2^Q)(\mathbf{w}) \\ &= (\varphi_1^Q(\mathbf{z}) - \gamma\varphi_1^Q(\mathbf{w})) + (\varphi_2^Q(\mathbf{z}) - \gamma\varphi_2^Q(\mathbf{w})) \\ &= U(\varphi_1^Q)([\mathbf{z}; \mathbf{w}]) + U(\varphi_2^Q)([\mathbf{z}; \mathbf{w}]), \forall \mathbf{z}, \mathbf{w} \in \mathcal{Z}, \end{aligned}$$

and

$$\begin{aligned} U(\alpha\varphi_1^Q)([\mathbf{z}; \mathbf{w}]) &= \alpha\varphi_1^Q(\mathbf{z}) - \gamma\alpha\varphi_1^Q(\mathbf{w}) = \alpha(\varphi_1^Q(\mathbf{z}) - \gamma\varphi_1^Q(\mathbf{w})) \\ &= \alpha U(\varphi_1^Q)([\mathbf{z}; \mathbf{w}]), \forall \alpha \in \mathbb{R}, \forall \mathbf{z}, \mathbf{w} \in \mathcal{Z}, \end{aligned}$$

from which the linearity holds. Therefore, it is sufficient to show that  $\ker(U) = 0$  [69]. For any  $\varphi^Q \in \ker(U)$ , we obtain

$$U(\varphi^Q)([\mathbf{z}; \mathbf{z}]) = (1 - \gamma)\varphi^Q(\mathbf{z}) = 0, \forall \mathbf{z} \in \mathcal{Z},$$

which implies that  $\varphi^Q = 0$ .

Next, we show that  $\mathcal{H}_{\Psi^Q}$  is an RKHS. The space  $\mathcal{H}_{\Psi^Q}$  with the inner product defined in (IV.4) is isometric to the RKHS  $\mathcal{H}_Q$ , and hence is a Hilbert space. Because  $\kappa^Q(\cdot, \mathbf{z}) -$

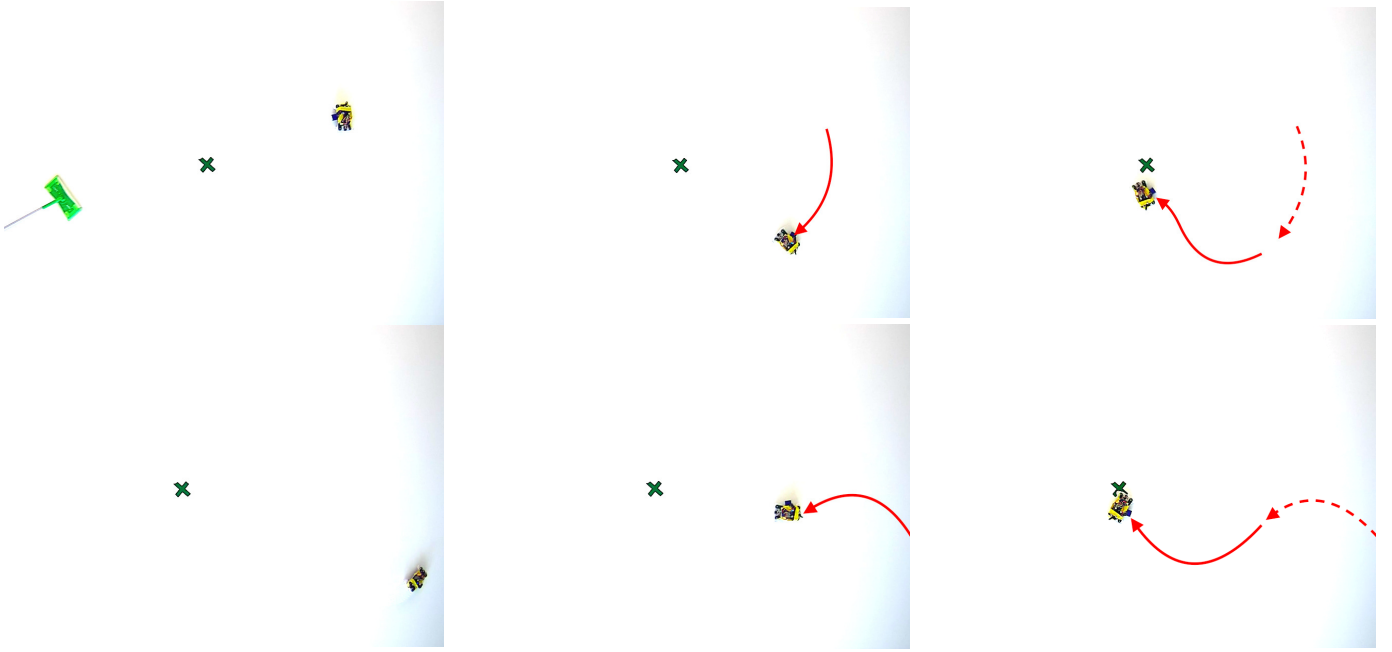


Fig. V.10. Two trajectories of the brushbot returning to the origin by using the action-value function saved at  $n = 1000$ . Red arrows show the trajectories. After being pushed away from the origin, the brushbot successfully returned to the origin again.

$\gamma\kappa^Q(\cdot, \mathbf{w}) \in \mathcal{H}_Q$ , it is true that  $\kappa(\cdot, [\mathbf{z}; \mathbf{w}]) \in \mathcal{H}_{\psi^Q}$ . Moreover, it holds that

$$\begin{aligned} & \langle \kappa(\cdot, [\mathbf{z}; \mathbf{w}]), \kappa(\cdot, [\bar{\mathbf{z}}; \bar{\mathbf{w}}]) \rangle_{\mathcal{H}_{\psi^Q}} \\ &= \langle \kappa^Q(\cdot, \mathbf{z}) - \gamma\kappa^Q(\cdot, \mathbf{w}), \kappa^Q(\cdot, \bar{\mathbf{z}}) - \gamma\kappa^Q(\cdot, \bar{\mathbf{w}}) \rangle_{\mathcal{H}_Q} \\ &= (\kappa^Q(\mathbf{z}, \bar{\mathbf{z}}) - \gamma\kappa^Q(\mathbf{w}, \bar{\mathbf{w}})) - \gamma(\kappa^Q(\mathbf{w}, \bar{\mathbf{z}}) - \gamma\kappa^Q(\mathbf{w}, \bar{\mathbf{w}})) \\ &= \kappa([\mathbf{z}; \mathbf{w}], [\bar{\mathbf{z}}; \bar{\mathbf{w}}]), \end{aligned}$$

and that

$$\begin{aligned} \langle \varphi, \kappa(\cdot, [\mathbf{z}; \mathbf{w}]) \rangle_{\mathcal{H}_{\psi^Q}} &= \langle \varphi^Q, \kappa^Q(\cdot, \mathbf{z}) - \gamma\kappa^Q(\cdot, \mathbf{w}) \rangle_{\mathcal{H}_Q} \\ &= \varphi^Q(\mathbf{z}) - \gamma\varphi^Q(\mathbf{w}) = \varphi([\mathbf{z}; \mathbf{w}]), \quad \forall \varphi \in \mathcal{H}_{\psi^Q}. \end{aligned}$$

Therefore,  $\kappa(\cdot, \cdot) : \mathcal{L}^2 \times \mathcal{L}^2 \rightarrow \mathbb{R}$  is the reproducing kernel with which the RKHS  $\mathcal{H}_{\psi^Q}$  is associated.

#### APPENDIX D PROOF OF COROLLARY IV.1

From the definition of the inner product in the RKHS  $\mathcal{H}_{\psi^Q}$ , it follows that

$$\begin{aligned} \left\| \hat{Q}_{n+1}^\phi - Q^{\phi*} \right\|_{\mathcal{H}_Q} &= \left\| \hat{\psi}_{n+1}^Q - \psi^{Q*} \right\|_{\mathcal{H}_{\psi^Q}} \\ &\leq \left\| \hat{\psi}_n^Q - \psi^{Q*} \right\|_{\mathcal{H}_{\psi^Q}} = \left\| \hat{Q}_n^\phi - Q^{\phi*} \right\|_{\mathcal{H}_Q}. \end{aligned}$$

#### APPENDIX E PROOF OF THEOREM IV.4

The line integral of  $\frac{\partial B(\mathbf{x})}{\partial \mathbf{x}}$  is path independent because it is the gradient of the scalar field  $B$  [70]. Let  $\mathbf{x}(t) := (1-t)\mathbf{x}_n + t\mathbf{x}_{n+1} = \mathbf{x}_n + t(\hat{f}_n(\mathbf{x}_n) + \hat{g}_n(\mathbf{x}_n)\mathbf{u}_n)$ , where  $t \in [0, 1]$  parameterizes the line path between  $\mathbf{x}_n$  and  $\mathbf{x}_{n+1}$ , then  $\frac{dB(\mathbf{x}(t))}{dt} =$

$\frac{\partial B(\mathbf{x}(t))}{\partial \mathbf{x}}(\hat{f}_n(\mathbf{x}_n) + \hat{g}_n(\mathbf{x}_n)\mathbf{u}_n)$ . Therefore, for any path  $A$  from  $\mathbf{x}_n$  to  $\hat{\mathbf{x}}_{n+1} := \mathbf{x}_n + \hat{f}_n(\mathbf{x}_n) + \hat{g}_n(\mathbf{x}_n)\mathbf{u}_n$ , it holds that

$$\begin{aligned} B(\hat{\mathbf{x}}_{n+1}) - B(\mathbf{x}_n) &= \int_A \frac{\partial B(\mathbf{x})}{\partial \mathbf{x}} \cdot d\mathbf{x} = \int_0^1 \frac{dB(\mathbf{x}(t))}{dt} dt \\ &\geq \int_0^1 \left( \frac{\partial B(\mathbf{x}_n)}{\partial \mathbf{x}} - vt(\hat{f}_n(\mathbf{x}_n) + \hat{g}_n(\mathbf{x}_n)\mathbf{u}_n)^\top \right) \\ &\quad (\hat{f}_n(\mathbf{x}_n) + \hat{g}_n(\mathbf{x}_n)\mathbf{u}_n) dt \\ &= \frac{\partial B(\mathbf{x}_n)}{\partial \mathbf{x}}(\hat{f}_n(\mathbf{x}_n) + \hat{g}_n(\mathbf{x}_n)\mathbf{u}_n) \\ &\quad - \frac{v}{2} \left\| \hat{f}_n(\mathbf{x}_n) + \hat{g}_n(\mathbf{x}_n)\mathbf{u}_n \right\|_{\mathbb{R}^{n_x}}^2. \end{aligned} \quad (\text{E.1})$$

The inequality implies that  $B(\hat{\mathbf{x}}_{n+1}) - B(\mathbf{x}_n)$  is greater than or equal to that in the case when  $\frac{\partial B(\mathbf{x})}{\partial \mathbf{x}}$  decrease along the line path at the maximum rate. Therefore, when (IV.10) is satisfied, it holds from (E.1) that

$$B(\hat{\mathbf{x}}_{n+1}) - B(\mathbf{x}_n) \geq -\eta B(\mathbf{x}_n) + \rho_1,$$

which is the control barrier certificate defined in (IV.1). Hence, (III.1) is satisfied by the same argument as in the proof of Theorem IV.1. Equation (IV.10) can be rewritten as

$$\begin{aligned} \frac{\partial B(\mathbf{x}_n)}{\partial \mathbf{x}}(\hat{f}_n(\mathbf{x}_n) + \hat{g}_n(\mathbf{x}_n)\mathbf{u}_n) \\ - \frac{v}{2} \left\| \hat{f}_n(\mathbf{x}_n) + \hat{g}_n(\mathbf{x}_n)\mathbf{u}_n \right\|_{\mathbb{R}^{n_x}}^2 \geq -\eta B(\mathbf{x}_n) + \rho_1. \end{aligned} \quad (\text{E.2})$$

The first term in the left hand side of (E.2) is affine to  $\mathbf{u}_n$ , the second term is the combination of a concave function  $-\frac{v}{2} \|\cdot\|_{\mathbb{R}^{n_x}}^2$  and an affine function of  $\mathbf{u}_n$ , which is concave. Therefore, the left hand side of (E.2) is a concave function, and the inequality (E.2) defines a convex constraint.



APPENDIX F  
KERNEL ADAPTIVE FILTER WITH MONOTONE  
APPROXIMATION PROPERTY

Kernel adaptive filter [25] is an adaptive extension of the kernel ridge regression [26], [27] or Gaussian processes. Multikernel adaptive filter [28] exploits multiple kernels to conduct learning in the sum space of RKHSs associated with each kernel. Let  $M \in \mathbb{Z}_{>0}$  be the number of kernels employed. Here, we only discuss the case that the dimension of the model parameter  $\mathbf{h}$  is fixed, for simplicity. Denote, by  $\mathcal{D}_m := \{\kappa_m(\cdot, \tilde{\mathbf{z}}_{m,j})\}_{j \in \{1,2,\dots,r_m\}}$ ,  $m \in \{1,2,\dots,M\}$ ,  $r_m \in \mathbb{Z}_{>0}$ , the time-dependent set of functions, referred to as a *dictionary*, at time instant  $n$  for the  $m$ th kernel  $\kappa_m(\cdot, \cdot)$ . The current estimator  $\hat{\Psi}_n$  is evaluated at the current input  $\mathbf{z}_n$ , in a linear form, as

$$\hat{\Psi}_n(\mathbf{z}_n) := \mathbf{h}_n^\top \mathbf{k}(\mathbf{z}_n) = \sum_{m=1}^M \mathbf{h}_{m,n}^\top \mathbf{k}_m(\mathbf{z}_n),$$

where  $\mathbf{h}_n := [\mathbf{h}_{1,n}; \mathbf{h}_{2,n}; \dots; \mathbf{h}_{M,n}] := [h_1; h_2; \dots; h_r] \in \mathbb{R}^r$ ,  $r := \sum_{m=1}^M r_m$ , is the coefficient vector, and  $\mathbf{k}(\mathbf{z}_n) := [\mathbf{k}_1(\mathbf{z}_n); \mathbf{k}_2(\mathbf{z}_n); \dots; \mathbf{k}_M(\mathbf{z}_n)] \in \mathbb{R}^r$ ,  $\mathbf{k}_m(\mathbf{z}_n) := [\kappa_m(\mathbf{z}_n, \tilde{\mathbf{z}}_{m,1}); \kappa_m(\mathbf{z}_n, \tilde{\mathbf{z}}_{m,2}); \dots; \kappa_m(\mathbf{z}_n, \tilde{\mathbf{z}}_{m,r_m})] \in \mathbb{R}^{r_m}$ . To obtain a sparse model parameter, we define the cost at time instant  $n$  as

$$\Theta_n(\mathbf{h}) := \frac{1}{2} \sum_{\iota=n-s+1}^n \frac{1}{s} \text{dist}^2(\mathbf{h}, C_\iota) + \mu \|\mathbf{h}\|_1, \quad (\text{F.1})$$

where  $\iota \in \{n-s+1, n\} \subset \mathbb{Z}_{\geq 0}$ ,  $s \in \mathbb{Z}_{>0}$ , and

$$C_\iota := \{\mathbf{h} \in \mathbb{R}^r \mid |\mathbf{h}^\top \mathbf{k}(\mathbf{z}_\iota) - \delta_\iota| \leq \varepsilon_1\}, \quad \varepsilon_1 \geq 0, \quad (\text{F.2})$$

which is a set of coefficient vector  $\mathbf{h}$  satisfying instantaneous-error-zero with a precision parameter  $\varepsilon_1$ . Here,  $(\mathbf{z}_n, \delta_n)$ ,  $\mathbf{z}_n \in \mathbb{R}^r$ ,  $\delta_n \in \mathbb{R}$  is the input-output pair at time instant  $n$ , and the  $\ell_1$ -norm regularization  $\|\mathbf{h}\|_1 := \sum_{i=1}^r |h_i|$  with a parameter  $\mu \geq 0$  promotes sparsity of  $\mathbf{h}$ . The update rule of the adaptive proximal forward-backward splitting [71], which is an adaptive filter designed for sparse optimizations, for the cost (F.1) is given by

$$\mathbf{h}_{n+1} = \text{prox}_{\lambda\mu} \left[ (1-\lambda)I + \lambda \sum_{\iota=n-s+1}^n \frac{1}{s} P_{C_\iota} \right] (\mathbf{h}_n),$$

where  $\lambda \in (0, 2)$  is the step size,  $I$  is the identity operator, and

$$\text{prox}_{\lambda\mu}(\mathbf{h}) = \sum_{i=1}^r \text{sgn}(h_i) \max\{|h_i| - \lambda\mu, 0\} \mathbf{e}_i,$$

where  $\text{sgn}(\cdot)$  is the sign function. Then, the strictly monotone approximation property [71]:  $\|\mathbf{h}_{n+1} - \mathbf{h}_n^*\|_{\mathbb{R}^r} < \|\mathbf{h}_n - \mathbf{h}_n^*\|_{\mathbb{R}^r}$ ,  $\forall \mathbf{h}_n^* \in \Omega_n := \text{argmin}_{\mathbf{h} \in \mathbb{R}^r} \Theta_n(\mathbf{h})$ , holds if  $\mathbf{h}_n \notin \Omega_n \neq \emptyset$ .

**Dictionary Construction:** If the dictionary is insufficient, we can employ two novelty conditions when adding the kernel functions  $\{\kappa_m(\cdot, \mathbf{z}_n)\}_{m \in \{1,2,\dots,M\}}$  to the dictionary: (i) the maximum-dictionary-size condition

$$r \leq r_{\max}, \quad r_{\max} \in \mathbb{Z}_{>0},$$

and (ii) the large-normalized-error condition

$$|\delta_n - \hat{\Psi}_n(\mathbf{z}_n)|^2 > \varepsilon_2 |\hat{\Psi}_n(\mathbf{z}_n)|^2, \quad \varepsilon_2 \geq 0.$$

By using sparse optimizations, *nonactive* structural components represented by some kernel functions can also be removed, and the dictionary is refined as time goes by. To effectively achieve a compact representation of the model, it might be required to appropriately weigh the kernel functions to include some preferences on a structure of the model. The following lemma implies that the resulting kernels are still reproducing kernels.

**Lemma F.1** ([29, Theorem 2]). Let  $\kappa : \mathcal{Z} \times \mathcal{Z} \rightarrow \mathbb{R}$  be the reproducing kernel of an RKHS  $(\mathcal{H}, \langle \cdot, \cdot \rangle_{\mathcal{H}})$ . Then,  $\tau\kappa(\mathbf{z}, \mathbf{w})$ ,  $\mathbf{z}, \mathbf{w} \in \mathcal{Z}$  for arbitrary  $\tau > 0$  is the reproducing kernel of the RKHS  $(\mathcal{H}_\tau, \langle \cdot, \cdot \rangle_{\mathcal{H}_\tau})$  with the inner product  $\langle \mathbf{z}, \mathbf{w} \rangle_{\mathcal{H}_\tau} := \tau^{-1} \langle \mathbf{z}, \mathbf{w} \rangle_{\mathcal{H}}$ ,  $\mathbf{z}, \mathbf{w} \in \mathcal{Z}$ .

APPENDIX G  
COMPARISON TO PARAMETRIC APPROACHES AND THE  
GAUSSIAN PROCESS SARSA

If the suitable set of basis functions for approximating action-value functions is available, we can adopt a parametric approach for action-value function approximation. Let an estimate of the action-value function at time instant  $n$  is given by  $\hat{Q}_n^\phi(\mathbf{z}) = \mathbf{h}_n^\top \zeta(\mathbf{z})$ , where  $\zeta : \mathcal{Z} \rightarrow \mathbb{R}^r$  is fixed for all time. In this parametric case, given an input-output pair  $([\mathbf{z}_n; \mathbf{z}_{n+1}], R(\mathbf{x}_n, \mathbf{u}_n))$ , we can update the estimate of the action-value function as

$$\hat{Q}_{n+1}^\phi = \mathbf{h}_n - \lambda [\mathbf{h}_n^\top (\zeta(\mathbf{z}_n) - \gamma\zeta(\mathbf{z}_{n+1})) - R(\mathbf{x}_n, \mathbf{u}_n)] \cdot (\zeta(\mathbf{z}_n) - \gamma\zeta(\mathbf{z}_{n+1})).$$

Then, stable tracking is achieved if the step size  $\lambda$  is properly selected, even after the dynamics or the policy is changed.

On the other hand, when employing a kernel-based learning, it is not trivial how to update the estimate in a theoretically formal manner. Because the output of the action-value function is not directly observable, the expansion  $\sum_{i=0}^n \kappa^Q(\cdot, \mathbf{z}_n)$  (where  $\kappa^Q$  is the reproducing kernel of the RKHS containing the action-value function) cannot be validated by the representer theorem [72] any more. By defining the RKHS  $\mathcal{H}_{\psi^Q}$  as in Theorem IV.3, however, we can view action-value function approximation as the supervised learning in the RKHS  $\mathcal{H}_{\psi^Q}$ , and can overcome the aforementioned issue. We mention that when an adaptive filter is employed in the RKHS  $\mathcal{H}_{\psi^Q}$ , we do not have to reset learning even after policies are updated or the dynamics changes, since the domain of  $\mathcal{H}_{\psi^Q}$  is  $\mathcal{Z} \times \mathcal{Z}$  instead of  $\mathcal{Z}$ . The example below indicates that our approach is general.

As discussed in Section II-A, the least squares temporal difference algorithm has been extended to kernel-based methods including the Gaussian process SARSA [35]. Given a set of input data  $\{\mathbf{z}_n\}_{n=0,1,\dots,N_d}$ ,  $\mathbf{z}_n := [\mathbf{x}_n; \mathbf{u}_n]$ ,  $N_d \in \mathbb{Z}_{>0}$ , the posterior mean  $m^Q$  and variance  $\mu^{Q^2}$  of  $\hat{Q}_{N_d}^\phi$  at a point  $\mathbf{z}_* \in \mathcal{Z}$  are given by

$$m^Q(\mathbf{z}_*) = \tilde{\mathbf{k}}_{N_d}^\top \mathbf{H}^\top (\mathbf{H} \mathbf{K}^Q \mathbf{H}^\top + \Sigma)^{-1} \mathbf{R}_{N_d-1}, \quad (\text{G.1})$$

$$\mu^{Q^2}(\mathbf{z}_*) = \kappa^Q(\mathbf{z}_*, \mathbf{z}_*) - \tilde{\mathbf{k}}_{N_d}^\top \mathbf{H}^\top (\mathbf{H} \mathbf{K}^Q \mathbf{H}^\top + \Sigma)^{-1} \mathbf{H} \tilde{\mathbf{k}}_{N_d}, \quad (\text{G.2})$$

where  $\mathbf{R}_{N_d-1} \sim \mathcal{N}([R(\mathbf{x}_0, \mathbf{u}_0); R(\mathbf{x}_1, \mathbf{u}_1); \dots; R(\mathbf{x}_{N_d-1}, \mathbf{u}_{N_d-1})], \Sigma)$  is the vector of immediate rewards,  $\kappa^Q$  is the reproducing kernel of  $\mathcal{H}_Q$ ,  $\tilde{\mathbf{k}}_{N_d} := [\kappa^Q(\mathbf{z}_*, \mathbf{z}_0); \kappa^Q(\mathbf{z}_*, \mathbf{z}_1); \dots; \kappa^Q(\mathbf{z}_*, \mathbf{z}_{N_d})]$ , the  $(i, j)$  entry of  $\mathbf{K}^Q \in \mathbb{R}^{(N_d+1) \times (N_d+1)}$  is  $\kappa^Q(\mathbf{z}_{i-1}, \mathbf{z}_{j-1})$ , and  $\Sigma \in \mathbb{R}^{N_d \times N_d}$  is the covariance matrix of  $\mathbf{R}_{N_d-1}$ . Here, the matrix  $\mathbf{H}$  is defined by

$$\mathbf{H} := \begin{bmatrix} 1 & -\gamma & 0 & \dots & 0 \\ 0 & 1 & -\gamma & \dots & 0 \\ \vdots & & & & \vdots \\ 0 & 0 & \dots & 1 & -\gamma \end{bmatrix} \in \mathbb{R}^{N_d \times (N_d+1)}.$$

If we employ a Gaussian process for learning  $\psi^Q$  in  $\mathcal{H}_{\psi^Q}$  defined in Theorem IV.3, the posterior mean  $m^{\psi^Q}$  and variance  $\mu^{\psi^Q}$  of  $\hat{\psi}_{N_d}^Q$  at a point  $[\mathbf{z}_*; \mathbf{w}_*] \in \mathcal{Z} \times \mathcal{Z}$  are given by

$$m^{\psi^Q}([\mathbf{z}_*; \mathbf{w}_*]) = \mathbf{k}_{N_d}^T (\mathbf{K} + \Sigma)^{-1} \mathbf{R}_{N_d-1},$$

$$\mu^{\psi^Q}([\mathbf{z}_*; \mathbf{w}_*]) = \kappa([\mathbf{z}_*; \mathbf{w}_*]; [\mathbf{z}_*; \mathbf{w}_*]) - \mathbf{k}_{N_d}^T (\mathbf{K} + \Sigma)^{-1} \mathbf{k}_{N_d},$$

where  $\mathbf{k}_{N_d} := [\kappa([\mathbf{z}_*; \mathbf{w}_*], [\mathbf{z}_0; \mathbf{z}_1]); \dots; \kappa([\mathbf{z}_*; \mathbf{w}_*], [\mathbf{z}_{N_d-1}; \mathbf{z}_{N_d}])]$ , and the  $(i, j)$  entry of  $\mathbf{K} \in \mathbb{R}^{N \times N}$  is  $\kappa([\mathbf{z}_{i-1}; \mathbf{z}_i], [\mathbf{z}_{j-1}; \mathbf{z}_j])$ . Then, the posterior mean  $m^Q$  and variance  $\mu^Q$  of  $\hat{Q}_{N_d}^Q$  at a point  $\mathbf{z}_* \in \mathcal{Z}$  are given by

$$m^Q(\mathbf{z}_*) = U^{-1}(m^{\psi^Q}(\cdot))(\mathbf{z}_*) = \mathbf{k}_{N_d}^Q{}^T (\mathbf{K} + \Sigma)^{-1} \mathbf{R}_{N_d-1},$$

$$\mu^Q(\mathbf{z}_*) = \kappa^Q(\mathbf{z}_*, \mathbf{z}_*) - \mathbf{k}_{N_d}^Q{}^T (\mathbf{K} + \Sigma)^{-1} \mathbf{k}_{N_d}^Q,$$

which result in the same values as (G.1) and (G.2).

## REFERENCES

- [1] R. S. Sutton and A. G. Barto, *Reinforcement learning: An introduction*. MIT Press, 1998.
- [2] F. L. Lewis and D. Vrabie, "Reinforcement learning and adaptive dynamic programming for feedback control," *IEEE Circuits and Systems Magazine*, vol. 9, no. 3, 2009.
- [3] D. Liberzon, *Calculus of variations and optimal control theory: a concise introduction*. Princeton University Press, 2011.
- [4] F. Berkenkamp, M. Turchetta, A. P. Schoellig, and A. Krause, "Safe model-based reinforcement learning with stability guarantees," in *Proc. NIPS*, 2017.
- [5] F. Berkenkamp, R. Moriconi, A. P. Schoellig, and A. Krause, "Safe learning of regions of attraction for uncertain, nonlinear systems with Gaussian processes," in *Proc. CDC*, 2016, pp. 4661–4666.
- [6] J. Schreiter, D. Nguyen-Tuong, M. Eberts, B. Bischoff, H. Markert, and M. Toussaint, "Safe exploration for active learning with Gaussian processes," in *Proc. ECML PKDD*, 2015, pp. 133–149.
- [7] A. K. Akametalu, J. F. Fisac, J. H. Gillula, S. Kaynama, M. N. Zeilinger, and C. J. Tomlin, "Reachability-based safe learning with Gaussian processes," in *Proc. CDC*, 2014, pp. 1424–1431.
- [8] S. Shalev-Shwartz, S. Shammah, and A. Shashua, "Safe, multi-agent, reinforcement learning for autonomous driving," *arXiv preprint arXiv:1610.03295*, 2016.
- [9] H. B. Ammar, R. Tutunov, and E. Eaton, "Safe policy search for lifelong reinforcement learning with sublinear regret," in *Proc. ICML*, 2015, pp. 2361–2369.
- [10] D. A. Niekirk, B. V. and B. Rosman, "Online constrained model-based reinforcement learning," in *Proc. AUAI*, 2017.
- [11] J. Achiam, D. Held, A. Tamar, and P. Abbeel, "Constrained policy optimization," in *Proc. ICML*, 2017.
- [12] P. Abbeel and A. Y. Ng, "Exploration and apprenticeship learning in reinforcement learning," in *Proc. ICML*, 2005, pp. 1–8.
- [13] L. Wang, E. A. Theodorou, and M. Egerstedt, "Safe learning of quadrotor dynamics using barrier certificates," *arXiv preprint arXiv:1710.05472*, 2017.
- [14] J. Garcia and F. Fernández, "A comprehensive survey on safe reinforcement learning," *J. Mach. Learn. Res.*, vol. 16, no. 1, pp. 1437–1480, 2015.
- [15] B. D. Argall, S. Chernova, M. Veloso, and B. Browning, "A survey of robot learning from demonstration," *Robotics and Autonomous Systems*, vol. 57, no. 5, pp. 469–483, 2009.
- [16] P. Geibel, "Reinforcement learning for MDPs with constraints," in *Proc. ECML*, vol. 4212, 2006, pp. 646–653.
- [17] S. P. Coraluppi and S. I. Marcus, "Risk-sensitive and minimax control of discrete-time, finite-state Markov decision processes," *Automatica*, vol. 35, no. 2, pp. 301–309, 1999.
- [18] C. E. Rasmussen and C. K. Williams, *Gaussian processes for machine learning*. MIT press Cambridge, 2006, vol. 1.
- [19] X. Xu, P. Tabuada, J. W. Grizzle, and A. D. Ames, "Robustness of control barrier functions for safety critical control," in *Proc. IFAC*, vol. 48, no. 27, 2015, pp. 54–61.
- [20] P. Wieland and F. Allgöwer, "Constructive safety using control barrier functions," in *Proc. IFAC*, vol. 40, no. 12, 2007, pp. 462–467.
- [21] P. Glotfelter, J. Cortés, and M. Egerstedt, "Nonsmooth barrier functions with applications to multi-robot systems," *IEEE Control Systems Letters*, vol. 1, no. 2, pp. 310–315, 2017.
- [22] L. Wang, A. D. Ames, and M. Egerstedt, "Safety barrier certificates for collisions-free multirobot systems," *IEEE Trans. Robotics*, 2017.
- [23] A. D. Ames, X. Xu, J. W. Grizzle, and P. Tabuada, "Control barrier function based quadratic programs with application to automotive safety systems," *arXiv preprint arXiv:1609.06408*, 2016.
- [24] A. Agrawal and K. Sreenath, "Discrete control barrier functions for safety-critical control of discrete systems with application to bipedal robot navigation," in *Proc. RSS*, 2017.
- [25] W. Liu, J. Principe, and S. Haykin, *Kernel adaptive filtering*. New Jersey: Wiley, 2010.
- [26] K. R. Müller, S. Mika, G. Ratsch, K. Tsuda, and B. Scholkopf, "An introduction to kernel-based learning algorithms," *IEEE Trans. Neural Networks*, vol. 12, no. 2, pp. 181–201, 2001.
- [27] B. Schölkopf and A. Smola, *Learning with kernels*. MIT Press, Cambridge, 2002.
- [28] M. Yukawa, "Multikernel adaptive filtering," *IEEE Trans. Signal Processing*, vol. 60, no. 9, pp. 4672–4682, Sept. 2012.
- [29] —, "Adaptive learning in Cartesian product of reproducing kernel Hilbert spaces," *IEEE Trans. Signal Processing*, vol. 63, no. 22, pp. 6037–6048, Nov. 2015.
- [30] O. Toda and M. Yukawa, "Online model-selection and learning for nonlinear estimation based on multikernel adaptive filtering," *IEICE Trans. Fundamentals of Electronics, Communications and Computer Sciences*, vol. 100, no. 1, pp. 236–250, 2017.
- [31] M. Ohnishi and M. Yukawa, "Online learning in  $L^2$  space with multiple Gaussian kernels," in *Proc. EUSIPCO*, 2017, pp. 1594–1598.
- [32] —, "Online nonlinear estimation via iterative  $l^2$ -space projections: Reproducing kernel of subspace," *IEEE Trans. Signal Processing*, vol. 66, no. 15, pp. 4050–4064, 2018.
- [33] L. Baird, "Residual algorithms: Reinforcement learning with function approximation," in *Proc. ICML*, 1995, pp. 30–37.
- [34] S. Mahadevan, B. Liu, P. Thomas, W. Dabney, S. Giguere, N. Jacek, I. Gemp, and J. Liu, "Proximal reinforcement learning: A new theory of sequential decision making in primal-dual spaces," *arXiv preprint arXiv:1405.6757*, 2014.
- [35] Y. Engel, S. Mannor, and R. Meir, "Reinforcement learning with Gaussian processes," in *Proc. ICML*, 2005, pp. 201–208.
- [36] D. Ormoneit and P. Glynn, "Kernel-based reinforcement learning in average-cost problems," *IEEE Trans. Automatic Control*, vol. 47, no. 10, pp. 1624–1636, 2002.
- [37] X. Xu, D. Hu, and X. Lu, "Kernel-based least squares policy iteration for reinforcement learning," *IEEE Trans. Neural Networks*, vol. 18, no. 4, pp. 973–992, 2007.
- [38] B. Bethke, J. P. How, and A. Ozdaglar, "Kernel-based reinforcement learning using Bellman residual elimination," in *MIT Working Paper*, 2008.
- [39] J. Kober, J. A. Bagnell, and J. Peters, "Reinforcement learning in robotics: A survey," *The International Journal of Robotics Research*, vol. 32, no. 11, pp. 1238–1274, 2013.
- [40] V. M. Janakiraman, X. L. Nguyen, and D. Assanis, "A Lyapunov based stable online learning algorithm for nonlinear dynamical systems using extreme learning machines," in *IEEE Proc. IJCNN*, 2013, pp. 1–8.
- [41] M. French and E. Rogers, "Non-linear iterative learning by an adaptive Lyapunov technique," *International Journal of Control*, vol. 73, no. 10, pp. 840–850, 2000.
- [42] M. M. Polycarpou, "Stable adaptive neural control scheme for nonlinear systems," *IEEE Trans. Automatic Control*, vol. 41, no. 3, pp. 447–451, 1996.

- [43] K. J. Åström and B. Wittenmark, *Adaptive control*. Courier Corporation, 2013.
- [44] C. A. Cheng and H. P. Huang, “Learn the Lagrangian: A vector-valued RKHS approach to identifying Lagrangian systems,” *IEEE Trans. Cybernetics*, vol. 46, no. 12, pp. 3247–3258, 2016.
- [45] M. Geist and O. Pietquin, “A brief survey of parametric value function approximation,” *Rapport Interne, Supélec*, 2010.
- [46] G. Taylor and R. Parr, “Kernelized value function approximation for reinforcement learning,” in *Proc. ICML*, 2009, pp. 1017–1024.
- [47] W. Sun and J. A. Bagnell, “Online Bellman residual and temporal difference algorithms with predictive error guarantees,” in *Proc. IJCAI*, 2016.
- [48] Y. Nishiyama, A. Boularias, A. Gretton, and K. Fukumizu, “Hilbert space embeddings of POMDPs,” *arXiv preprint arXiv:1210.4887*, 2012.
- [49] S. Grunewalder, G. Lever, L. Baldassarre, M. Pontil, and A. Gretton, “Modelling transition dynamics in MDPs with RKHS embeddings,” in *Proc. ICML*, 2012.
- [50] A. Barreto, D. Precup, and J. Pineau, “Practical kernel-based reinforcement learning,” *The Journal of Machine Learning Research*, vol. 17, no. 1, pp. 2372–2441, 2016.
- [51] A. S. Barreto, D. Precup, and J. Pineau, “Reinforcement learning using kernel-based stochastic factorization,” in *Proc. NIPS*, 2011, pp. 720–728.
- [52] B. Kveton and G. Theodorou, “Kernel-based reinforcement learning on representative states,” in *Proc. AAAI*, 2012.
- [53] J. Bae, P. Chhatbar, J. T. Francis, J. C. Sanchez, and J. C. Principe, “Reinforcement learning via kernel temporal difference,” in *IEEE Proc. EMBC*, 2011.
- [54] J. Reisinger, P. Stone, and R. Miikkulainen, “Online kernel selection for bayesian reinforcement learning,” in *Proc. ICML*, 2008, pp. 816–823.
- [55] Y. Cui, T. Matsubara, and K. Sugimoto, “Kernel dynamic policy programming: Applicable reinforcement learning to robot systems with high dimensional states,” *Neural Networks*, vol. 94, pp. 13–23, 2017.
- [56] H. Van H., J. Peters, and G. Neumann, “Learning of non-parametric control policies with high-dimensional state features,” in *Artificial Intelligence and Statistics*, 2015, pp. 995–1003.
- [57] J. A. Boyan, “Least-squares temporal difference learning,” in *Proc. ICML*, 1999, pp. 49–56.
- [58] R. S. Sutton, H. R. Maei, and C. Szepesvári, “A convergent  $O(n)$  temporal-difference algorithm for off-policy learning with linear function approximation,” in *Proc. NIPS*, 2009, pp. 1609–1616.
- [59] L. Wang, D. Han, and M. Egerstedt, “Permissive barrier certificates for safe stabilization using sum-of-squares,” *arXiv preprint arXiv:1802.08917*, 2018.
- [60] N. Aronszajn, “Theory of reproducing kernels,” *Trans. Amer. Math. Soc.*, vol. 68, no. 3, pp. 337–404, May 1950.
- [61] I. Steinwart, “On the influence of the kernel on the consistency of support vector machines,” *J. Mach. Learn. Res.*, vol. 2, pp. 67–93, 2001.
- [62] Z. P. Jiang and Y. Wang, “A converse Lyapunov theorem for discrete-time systems with disturbances,” *Systems & Control Letters*, vol. 45, no. 1, pp. 49–58, 2002.
- [63] A. Berlinet and A. C. Thomas, *Reproducing kernel Hilbert spaces in probability and statistics*. Kluwer, 2004.
- [64] M. L. Puterman and S. L. Brumelle, “On the convergence of policy iteration in stationary dynamic programming,” *Mathematics of Operations Research*, vol. 4, no. 1, pp. 60–69, 1979.
- [65] D. P. Bertsekas, *Dynamic programming and optimal control*. Athena Scientific Belmont, MA, 2005, vol. 1, no. 3.
- [66] D. Pickem, P. Glotfelter, L. Wang, M. Mote, A. Ames, E. Feron, and M. Egerstedt, “The robotarium: A remotely accessible swarm robotics research testbed,” in *IEEE Proc. ICRA*, 2017, pp. 1699–1706.
- [67] H. Q. Minh, “Some properties of Gaussian reproducing kernel Hilbert spaces and their implications for function approximation and learning theory,” *Constructive Approximation*, vol. 32, no. 2, pp. 307–338, 2010.
- [68] R. A. Ryan, *Introduction to tensor products of Banach spaces*. Springer Science & Business Media, 2013.
- [69] G. Strang, *Introduction to linear algebra*. Wellesley-Cambridge Press Wellesley, MA, 1993, vol. 3.
- [70] L. V. Ahlfors, “Complex analysis: an introduction to the theory of analytic functions of one complex variable,” *New York, London*, p. 177, 1953.
- [71] Y. Murakami, M. Yamagishi, M. Yukawa, and I. Yamada, “A sparse adaptive filtering using time-varying soft-thresholding techniques,” in *Proc. IEEE ICASSP*, 2010, pp. 3734–3737.
- [72] G. Kimeldorf and G. Wahba, “Some results on Tchebycheffian spline functions,” *Journal of Mathematical Analysis and Applications*, vol. 33, no. 1, pp. 82–95, 1971.